Print ISSN: 0976-2876 Online ISSN: 2250-0138

Available online at: http://www.ijsr.in

INDIAN JOURNAL OF SCIENTIFIC RESEARCH

DOI:10.32606/IJSR.V15.I1.00002

Received: 25-06-2024 Accepted: 04-07-2024 Publication: 31-08-2024

Indian J.Sci.Res. 15 (1): 09-30, 2024 Original Research Article

FORMULATION AND *In vitro* EVALUATION OF LIQUISOLID COMPACT OF CELECOXIB

EZEGBE CHEKWUBE ANDREW[a1], ANIKWE CELESTINE CHIDERA[b], OKORIE JAMES EKEMEZIE[c], OKAFOR NNEDIMMA PAULINE[d], AMARACHI GRACE EZEGBE[e], NWANKWO EMMANUEL CHINEDU[f] AND ONUNKWO CHUKWUNWIKE GODSWILL[g]

[acdfg]Department of Pharmaceutical Technology and Industrial Pharmacy, University of Nigeria, Nsukka, Nigeria

[b]Department of Pharmaceutics, University of Hertfordshire, England, United Kingdom

[e]Department of Home Science and Management, University of Nigeria, Nsukka, Nigeria

ABSTRACT

The liquisolid technique presents a promising avenue for enhancing the dissolution rate and bioavailability of poorly water-soluble drugs like celecoxib. This study investigated the formulation and evaluation of celecoxib tablets using this technique. Celecoxib tablets were prepared using the liquid-solid technique by incorporating a non-volatile liquid medication carrier and a suitable solid carrier. Various formulations were developed by altering the ratios of drug, carrier, and coating materials. The prepared tablets were characterized for their physical properties, drug content uniformity, *in vitro* dissolution behavior, and compatibility using Fourier-transform infrared (FTIR) spectroscopy. The solubility profile showed that the maximum rate of solubility was recorded in PEG-400 (11.03 ± 0.01) when compared to other non-volatile solvents. The angle of slide, indicated that the excipients used were within the acceptable limit of 33°. The FTIR spectroscopy showed compatibility of the drug and excipients. The results of the SEM showed that spherically-shaped vesicles were formed. Evaluation of the pre-compression parameters indicated that the drug content was highest in batch F-11 hence its optimization (96.1 ± 0.90). The post compression evaluation indicated that the official tests were within the acceptable range for disintegration time (2.25 ± 0.35). The results of the *in vitro* release studies of the optimized formulation, conventional tablet and reference commercial tablet showed that the amount of drug released increased steadily with time over the 1-hour period. Our findings underscore its viability as a strategy to enhance the therapeutic efficacy of poorly water-soluble drugs, offering promising prospects for pharmaceutical formulation.

KEYWORDS: Liquisolid, Celecoxib, Carrier, Coating Material, Dissolution

The pharmaceutical liquisolid technique has emerged as a promising approach for addressing the challenges associated with poorly water-soluble drugs. The solubility and bioavailability of drugs play a pivotal role in determining their therapeutic efficacy (Modi and Tayade, 2006). Poorly water-soluble drugs often encounter challenges related to achieving adequate plasma concentrations and desired pharmacological responses. Enhancing drug solubility and bioavailability is crucial for improving therapeutic outcomes, reducing the burden on patients, and optimizing the performance of pharmaceutical formulations (Allen and Cullis, 2004).

The liquisolid technique involves the conversion of liquid drugs or drug solutions into free-flowing, compressible powder blends (Amidon *et al.*, 1995). This transformation is achieved through the incorporation of drug solutions or suspensions into suitable carrier and coating materials, resulting in the formation of liquisolid compacts (Badawy *et al.*, 2016). The fundamental principles underlying this technique encompass the use of non-volatile solvents, carrier materials, and coating materials to achieve enhanced drug dissolution and absorption characteristics.

The formulation process for developing liquisolid systems involves the selection of suitable carrier and coating materials, as well as meticulous attention to factors influencing the stability and performance of liquisolid formulations. Characterization techniques are employed to evaluate the physical and chemical properties of liquisolid systems, ensuring the quality and effectiveness of the formulations (Chuahan *et al.*, 2012). The versatility of the pharmaceutical liquisolid technique extends to diverse applications in drug delivery. From poorly water-soluble drugs to highly potent compounds, the liquisolid approach offers a viable means of improving drug solubility and bioavailability. Furthermore, the potential for taste masking, modified release, and pediatric formulations further expands the scope of liquisolid applications (Farheen *et al.*, 2015). Continual advancements in pharmaceutical liquisolid systems have spurred a multitude of research endeavors aimed at refining and expanding the utility of this

[1]Corresponding author

technique. Novel excipients, innovative processing methods, and the integration of advanced technologies have emerged as key focal points in current research trends. Furthermore, the exploration of personalized medicine and tailored liquisolid formulations signifies a paradigm shift in drug development and formulation strategies (Sahil *et al.*, 2018). The pharmaceutical liquisolid technique represents a compelling avenue for addressing the formulation challenges associated with poorly water-soluble drugs. Its inherent advantages, coupled with ongoing research innovations, position liquisolid systems as pivotal contributors to advancing drug solubility, bioavailability, and patient-centric drug delivery. As the pharmaceutical industry continues to embrace innovation and scientific exploration, the evolution of liquisolid technology is poised to catalyze transformative developments in drug formulation and therapeutic outcomes (Kaur *et al.*, 2013). The Liquisolid technique is a revolutionary approach in pharmaceutical formulation that has garnered significant attention for its potential to address the challenges associated with poorly water-soluble drugs. This innovative method involves the conversion of liquid medications, such as solutions or suspensions of water-insoluble drugs, into free-flowing and compressible powders by blending them with specific powder excipients and non-volatile liquid vehicles. The Liquisolid technique has diverse applications in pharmaceutics, offering advantages such as enhanced drug solubility, improved dissolution rate, and controlled drug release. Due to the difficulty associated with poorly soluble or water insoluble drugs in terms of solubility, dissolution and bioavailability, there is need to formulate a liquisolid dosage form of this drug to bridge the gap (McCormack, 2011). The problem of poor solubility exhibited by class II and IV drugs have been a major challenging issue for the industry especially during the development of ideal solid dosage form. The aim of this research was to formulate and evaluate liquisolid tablets of celecoxib for enhanced solubility, dissolution, bioavailability and improved therapeutic application in the treatment and management of fever, mild to moderate pain and inflammation.

MATERIALS AND METHODS

Celecoxib (CLX1073/11/21) was purchased from Emzor Pharmaceuticals Ltd, Lagos. Polysorbate 80, PEG-4000 were purchased from (Sigma Aldrich, Kosher, USA). Colloidal silicon dioxide (Aerosil X50) was obtained from (Evonik, Germany). Lactose and sodium starch glycolate were obtained from DFE Pharma, UK), sorbitol was obtained from (TCI, USA). microcrystalline cellulose (MCC) and magnesium stearate were obtained from (Central drug house (P) Ltd, New Delhi, India). Methanol was obtained from (Astron Chemicals, Ahmedabad). Glycerin and sodium hydroxide were provided by (Mingtai Chemical Taiwan). Distilled water was obtained from (UNN Water Resources Management Laboratories Ltd; UNN, Enugu State, Nigeria).

Solubility Studies

The solubility of celecoxib was determined in various lipophilic solvents (Phosphate buffer pH 6.8, pH 7.4, 0.1N HCl, Tween 80, Propylene glycol, Polyethylene glycol (PEG-400 and distilled water). Saturated solutions were prepared by adding excess drug (5 g) to the vehicles (1 ml). Excess drug was stirred in above solvent, then sonicated for thirty minutes and kept for 24 hours. After this period, the solutions were filtered, diluted and analysed by UV spectrophotometer. Three determinations were carried out for each drug sample to calculate the solubility of the drug at 252 nm (Bettini *et al.*, 2001).

Drug-Excipient Compatibility Study (FTIR Spectroscopy)

Infra-red spectra of pure drug, carrier and coating materials were obtained by (Shimadzu 8400S Japan) FT-IR spectrometer. The samples were previously ground and mixed thoroughly with potassium bromide, an infra-red transparent matrix at 1:5 (sample: KRr) ratio respectively. The KBr discs were prepared by compressing the powders at a pressure of 5 tons for 5 mins in a hydraulic press. The scans were obtained at a resolution of 4 cm^{-1} from 4000 to 400 cm^{-1} (Dorozynski *et al.*, 2004).

Flowable Liquid-Retention Potential (Ø value) of the Excipients

Determination of the Angle of Slide

The carrier and coating material were weighed out accurately and placed at one end of a metal plate with a polished surface. The end was raised gradually until the plate made an angle with the horizontal at which was a measure for the flow characters of powders (Hoffman *et al.*, 2004).

Step I **Step II** **Step III**

Figure 1: Angle of slide measurement

Determination of Flowable Liquid-Retention Potential (Ø Value)

To the log of excipients, increasing amount of liquid vehicle were added and mixed well. The excipients adsorbed liquid vehicle resulting in a change in its flow properties. At each concentration of liquid vehicle added, the angle of slide Θ for excipients were re-determined as stated above. The corresponding Ø angle was calculated from the following equation.

$$\text{Ø value} = \frac{\text{weight of liquid}}{\text{weight of solid}} \quad (1)$$

The Ø values were plotted graphically against the corresponding angles of slide (h). The Ø value corresponding to an angle of slide 33^{o} represented the flowable liquid-retention potential of excipients (NICE, 2013).

Determination of the Liquid Load Factor (L_f)

A powder is known to retain certain limited amount of liquid medication, while maintaining an acceptable limit of flowability and compressibility. There are established mathematical models used to calculate the amount of liquid that can be loaded into the powder which would result into an acceptably free flowing and readily compressible dry looking powder (Sahil *et al.*, 2018).

$$Lf\omega = Ø + \omega/R \quad (2)$$

Ø: Flowable liquid retention potential of carrier.

ω: Flowable liquid retention potential of coating material.

R = Carriers and coating material ratio.

$$R = \frac{Q}{q}\ Q = \text{Carrier weight, q = coat weight.} \quad (3)$$

Weight of carrier and coating material can be calculated by the equation

$$L_{fo} = \frac{\text{weight of liquid medication (W) } (drug+non-volatile\ solvent)}{\text{Carrier weight (Q)}} \quad (4)$$

L_{fo} = Optimal liquid load factor.

Procedure for Preparation of Liquisolid System

Several celecoxib liquisolid formulations were prepared in batches of 100 tablets at different ratios of (1:1, 1:2, 1:3 and 1:4) drug: liquid vehicle. Calculated quantities of the drug and non-volatile solvent were accurately weighed in a 20-ml glass beaker and then mixed well. The resulting medication was incorporated into calculated quantities of carrier and coating materials. The mixing process was carried out in three steps:

In the first, the system was blended at an appropriate mixing rate of one rotation per second for approximately one minute in order to evenly distribute liquid medication in the powder.

In the second, the liquid/powder admixture was evenly spread as a uniform layer on the surface of a mortar and left standing for approximately 5 mins to allow the drug solution to be absorbed inside powder particles.

In the third, the powder was scraped off the mortar surface using an aluminum spatula. Subsequently carrier: coating material was added to this mixture and blended in a mortar. Starch (5% w/w) was added as a disintegrant and magnesium stearate (1% w/w) was added as a lubricant. Final formulation was compressed into tablets using a 12 mm single punch tablet compression machine (Syed and Pavani, 2012).

Procedure for Preparation of Directly Compressed Tablets (DCTs)

Celecoxib conventional tablets were produced by mixing the drug with the actual quantities of carrier and coating materials, for a period of 10 mins in a cubic mixer (Erweka, Germany). The mixture was then mixed with starch as disintegrating agent for 10 mins and then magnesium stearate (1%) was mixed for 5 mins. The final mixture was compressed using the tablet punching machine (Beignon *et al.*, 1998).

Pre-compression Evaluation of Powder Blend

Angle of Repose

Angle of repose is defined as the maximum angle possible between the surface of a pile of the powder and the horizontal plane. A plastic funnel in ring-supported by a retort stand. A sheet of paper was placed below the funnel assembly. A sheet of fibre board was placed below the funnel orifice making sure it fits tightly. A given quantity of the powder (30 g) was transferred into the funnel. The fibre sheet was drawn away and the timer simultaneously started. The timer was stopped when all of the powder had passed through the funnel. The height of the heap was measured using a graduated ruler. A pencil was used to outline the base of the contour. The angle of the conical heap so formed was determined from equation 5. The powder was returned to the funnel and the experiment was repeated thrice (ASTM International, 2013):

$$\text{Tan } \Theta = \frac{\text{height of powder heap,(h)}}{\text{radius of powder heap,(r)}} \quad (5)$$

Bulk Density

This is the ratio between given mass of powder and its bulk volume. A weighed quantity of powder (30.0 g) was placed in a 100-ml graduated cylinder. The cylinder was gently dropped onto a wooden surface three times from a height of one inch at 2 sec interval. The volume assumed after the treatment was taken as the bulk volume. The experiment was repeated thrice:

$$\text{Bulk density (g/ml)} = \frac{mass}{bulk\ volume} \quad (6)$$

Tapped Density

This is the ratio between given mass of powder and its bulk volume. A weighed quantity (30.0 g) of the powder was placed in a 100-ml graduated cylinder. The cylinder was tapped up to 500 times on the wooden surface or to a constant volume. The final volume attained represents the tapped volume. The experiment was repeated thrice:

$$\text{Tapped density (g/ml)} = \frac{mass}{tapped\ volume} \quad (7)$$

Carr's Index

This is used to access the flowability of a powder. The Carr's compressibility index (CI %) was calculated from the poured (bulk density) and tapped densities. CI was calculated using the following equation:

$$\text{Carr's index} = \frac{Tapped\ density - bulk\ density}{Tapped\ density} \text{ x } 100 \quad (8)$$

Hausner's Ratio

The Hausner ratio (HR), defined as the ratio of tapped to bulk densities. It is a common technique widely used to describe the packing behavior of powders when they are subjected to tapping.

$$\text{Hausner's ratio} = \frac{\text{tapped density}}{\text{bulk density}} \quad (9)$$

Drug Content

The powder blend containing 10 mg equivalent of drug was weighed and dissolved in methanol, and the volume was made up to 100 ml with distilled water. From the above solution, 10 ml was taken and diluted with distilled water. The absorbance of resulting solution was measured at 252 nm for celecoxib using the spectrophotometer (Spectumlab 725S, Hitachi Japan).

Post Compressional Evaluation of Liquisolid Tablets

General Appearance

The formulated tablets were evaluated for organoleptic properties such as colour, odour, taste and appearance.

Thickness

Ten (10) tablets were randomly selected from each formulation and thickness was measured individually by Vernier caliper.

Hardness

Ten (10) tablets were randomly selected from each batch. Using the Monsanto hardness tester (Praveen Enterprises, Bangalore), the pointer was fixed at 0 Kgf. One tablet was held and placed with the tester holder and the screw adjusted until the pressure applied cracked the tablet. The hardness of each tablet was determined and recorded.

Friability Test

Ten (10) tablets were selected at random from each batch. Subsequently, they were dedusted and accurately weighed together in an analytical balance. The dedusted tablets were then placed into the friabilator which was set to rotate at 25 rpm for 4 min. Then the tablets were removed, dedusted and re-weighed. The mean loss in weight and percent friability was then calculated. The friability test was repeated 3 times. The mean and standard deviation were then calculated.

$$\text{Friability test} = \frac{\text{initial weight} - \text{final weight}}{\text{initial weight}} \text{ x } 100 \quad (10)$$

Uniformity of Weight Test

Twenty (20) tablets were randomly selected from each batch. Using the analytical balance (120-5DM, S. Mettler, Germany), the 20 tablets were weighed together. The mean tablet weight was then calculated.

Subsequently the tablets were weighed individually and the weights of the tablets recorded. The variations of individual tablet weights from the mean weight were determined, and the percentage deviations calculated:

$$\text{Percentage deviation} = \frac{\text{Deviation}}{\text{Mean weight}} \text{ x } 100 \qquad (11)$$

Drug Content

The total amount of drug present in the liquisolid formulation was evaluated using UV-spectrophotometric analysis. Approximately weighed quantity of 10 mg equivalent of drug was taken from liquisolid formulation which was dissolved in 10 ml of methanol and the volume was made up to 100 ml with distilled water. From the above solution, 10 ml was taken and diluted with distilled water. The absorbance of resulting solution was measured at 252 nm for celecoxib using Spectrophotometer (Shimadzu UV-1700 Pharma Spec, Japan) and the drug content was calculated from the standard curve using the formula.

$$\text{Drug content} = \frac{\text{Sample absorbance}}{\text{Standard absorbance}} \text{x } 100 \qquad (12)$$

Disintegration Test

Six (6) tablets were selected at random from each batch using the Erweka disintegrating unit and distilled water as the disintegrating medium maintained at 37 ± 1.0 ^{o}C. One tablet was placed into each tube of the disintegrating unit. The time taken for each tablet to completely break down to particles and pass through the wire mesh was recorded. The mean disintegration time and standard deviation from each batch was calculated.

***In vitro* Release Studies**

The *in vitro* release studies was performed by using type II paddle dissolution apparatus in 900 ml of distilled water maintained at 37 ^{o}C ±0.5 ^{o}C and rotation speed of 50 rpm. All batches of tablets were evaluated in gastrointestinal release medium (0.1 N HCl, pH 1.2) for one hour. Samples (5ml) were withdrawn at suitable time intervals (5, 10, 15, 20, 25, 30, 45, and 60) minutes and filtered through 0.45 micron Whatman filter paper. Sink conditions were maintained throughout the study. The withdrawn samples were analysed by uv-visible spectrophotometer (Shimadzu uv-1700 Pharma Spec, Japan) at λmax of 252 nm for celecoxib. The studies were done in triplicates (Utsav and Khushbu, 2018).

***In vitro* Drug Release Kinetics**

Various kinetic models were used to describe the *in vitro* release kinetics and mechanisms of drug release from the liquisolid tablets. The zero-order kinetics explains the systems where the drug release rate is independent of its concentration (eqn. 13). The first order kinetics is used to describe the release from systems where the release rate is dependent on concentration (eqn. 14). Higuchi model describes the release of drugs from the insoluble matrix as a square root of time (eqn. 15). Korsmeyer is used to describe the drug release from a polymeric system (eqn. 16) (Ankit *et al.*, 2013):

$$C_o - C_t = K_o t$$

$$C_t = C_o + K_o t \qquad (13)$$

C_t is the amount of drug released at time t,

C_o is the initial concentration of drug at time t = 0,

K_o is the zero-order rate constant.

$$\text{Log } C = \log C_o - K_1 t/2.303 \qquad (14)$$

K_t is the first order rate equation expressed in time $^{-1}$ or per hour, C_o is the initial concentration of the drug, C is the percent of drug remaining at time t

$$ft = Q = KH.\ t_{1/2} \qquad (15)$$

where, Q is the amount of drug released in time t per unit area, KH is the Higuchi dissolution constant

$$Mt / M\infty = K_{kp} t^n \qquad (16)$$

where, Mt / M∞ is a fraction of drug released at time t, K_{kp} is the Korsmeyer release rate constant and n is the release exponent. The n value is used to characterize different release for cylindrical shaped matrices and the value of n characterizes the release mechanism of drug.

Powder x-ray Diffraction Studies

Powder x-ray diffraction pattern of celecoxib, carrier and coating material were studied using the x-ray diffractometer (XRD-462, Digaku, Japan). Voltage and current were set at 40 KV and 30 mA respectively. All pattern scanned over range 5-70^{o} 2Θ angle with a scan speed of 10 ^{o}/min (Akinlade *et al.*, 2010).

Selection and Evaluation of Optimized Formulation

The optimized formulation was selected on the results obtained from solubility studies in various non-volatile solvents, drug content and *in vitro* release studies. Comparison with directly compressed and liquisolid formulated tablets.The *in vitro* release of optimized formulation was compared with directly compressed tablets. Infrared spectroscopic studies for optimized formulation (Same procedure mentioned in compatibility studies was carried out)

Differential Scanning Colorimetry (DSC) Studies for Optimized Formulation

Thermal curves of pure drug, carrier, coating material and optimized formulation were recorded by simultaneous differential scanning calorimeter (DSC Q 200 V 24.4 Build 116). Each sample (approximately 2.5 mg) were scanned in hermetic pan made of aluminum at heating rate of 10°C/min over the range of 50°C -220°C with an empty aluminum pan used as reference. Samples were heated under nitrogen atmosphere (flow rate of N2-50 ml/min) (Asare-Addo *et al.*, 2013).

SEM Analysis for Optimized Formulation

Scanning electron microscopy was used to assess the morphological characteristics of the final liquisolid compacts. The samples were fixed on aluminum stubs with double-sided tape, gold coated sputter examined in the microscope using an accelerating voltage of 15 kv at a working distance of 8 mm and magnification of x10000.

Formulation Design

Design Expert® 12.0 software was used to create formulation design for the purpose of optimization of liquisolid tablets. Two independent factors were used to suit the experimental needs viz. concentration of the nonvolatile solvent and carrier: coat ratio (R). Dependent factors used were drug release (%), angle of repose (^{o}). Central composite randomized design was applied to screen via response surface methodology. Response 1 and 2 was evaluated by quadratic model and Response 3 by linear model by ANOVA. The estimations for the cumulative drug release and angle of repose were set at the ranges of 80-99% and 25-35^o respectively.

Data Analysis

All the measurements were repeated at least thrice and the data obtained analyzed by Student *t*-test and One-Way Analysis of Variance (ANOVA). Statistical analysis was performed using Statistical Product and Services Solution software (SPSS, version 22.0 Inc., Chicago IL, USA) and Excel Microsoft Office version 2012. The results were presented as mean ± SD, and statistical differences between means considered significant at ($p < 0.05$).

RESULTS AND DISCUSSION

Solubility Profile of Celecoxib in Various Solvents

The solubility profile of celecoxib indicated that the drug is practically insoluble in water (0.05 mg/ml). Minimal solubility was recorded in acidic environment (0.1 N HCl). The non-volatile solvent that gave the highest degree of solubility was PEG 400, thus it was used as the solvent of choice in the formulation of celecoxib liquisolid tablets (Table 1).

According to Alireza H *et al*, the results of the solubility studies indicated that pure celecoxib had very low solubility in water at 25°C (3 ± 0.68 µg/ml) (Alireza *et al.*, 2015).

Table 1: Solubility profile of Celecoxib in various solvents

Solvent/vehicle	Celecoxib
Distilled water	0.05 ± 0.01
Tween-80	11.03 ± 0.01
PEG 400	13.10 ± 0.36
Propylene glycol	10.07 ± 0.02
Glycerin	08.02 ± 0.33
Methanol	4.11 ± 0.39
Glacial acetic acid	2.08 ± 0.06
Buffer pH 7.4	2.01 ± 0.02
Buffer pH 6.8	2.10 ± 0.28
0.1N HCl.	01.09 ± 0.35

Liquid Retention Potential and Liquid Load Factor

At a given ratio of 1/R, different L_f was obtained and graph of L_f against 1/R was given.

From the graph equation Y = 0.3185 + 1.4604 X and it was compared to Lf = Lfω = Ø + ω (1/R) where Ø is the liquid retention potential of carrier and ω is the liquid retention potential of coating material. Thus the flowable liquid retention potential of carrier and coating material was found to be 0.3185 and 1.4604 respectively.

Angle of Slide for API, Carrier and Coating Materials

Table 2 depicted the angle of slide for the active ingredient, carrier and coating materials. Angle of slide indicates the flow property of powder compact. Increase in carrier coating ratio leads to an increase in angle of slide which indicates poor flow property (Armstrong, 2006). For liquisolid powders 33^o is considered optimum and acceptable angle. The flow properties of powders are very crucial in efficient tableting operation. It ensures efficient mixing and acceptable weight uniformity for the compressed tablets. The essence of determining the angle of slide is to help identify drugs that are poorly flowable at the pre-formulation stage. This problem can be solved by selecting appropriate excipients. Table 2 indicated that the carrier materials (maize starch and lactose) had an angle of slide at 33.0 ± 1.4 and 33.0 ± 0.00 respectively, thus signifying an optimum and acceptable angle. The coating material (SiO_2) had an angle of slide at 33.5 ± 0.35, while magnesium stearate (lubricant) had an

acceptable angle of slide at 33.0 ± 2.83. Celecoxib had an angle of slide at 36.0 ± 0.71. This value was above the acceptable angle of 33^{o}, thus the need to select appropriate excipients to handle the poor flowability of the drug at the pre-formulation stage.

Table 2: Pre-compression parameter of formulation (Angle of slide)

Drug/excipient	Angle of slide (^{o}) (mean ± SD)
Maize starch	33.0 ± 1.40
Lactose	33.0 ± 0.00
Magnesium stearate	33.0 ± 2.83
Microcrystalline cellulose	32.0 ± 2.12
Celecoxib	36.0 ± 0.71
Silicon dioxide (SiO_2)	33.5 ± 0.35

FTIR Spectroscopy (Drug- Excipient Compactibility Studies)

Figure 2 shows the characteristic peaks of celecoxib at 3819.7, 3211.5, 2590.9, 1880.6 and 1347.4 cm^{-1} corresponding to -OH, -NH single bond stretch, C-H single bong stretch, nitriles, C=O, C=C and C=N and C-O, C-N, C-C single bond stretch respectively. According to Gulshan *et al*; celecoxib showed characteristic peaks at 1159 cm^{-1} due to S=O stretching, 3338 cm^{-1} to NH_2 stretching and 1563 cm^{-1} due to N-H stretching (Gulshan *et al.*, 2016).

Figure 3 shows the characteristics peaks of microcrystalline cellulose at 3925.2, 3245.2, 2582.1, 1997.8 and 1468.4 cm^{-1} corresponding to O-H, N-H single bond stretch, C-H single bond stretch, carbenes triple bond, C=O, C=C double bond and C-C, C-O single bond respectively. According to Ning *et al.* (2011), the spectrum of MCC showed characteristic peaks at 3390 and a band at 1636 cm^{-1} corresponding to the stretching and bending modes of the surface hydroxyls. The peak at 2905 cm^{-1} belongs to the asymmetrically stretching vibration of C-H in a pyramid ring and the broad absorption peak at 1059 cm^{-1} is attributed to the C-O of cellulose.

Figure 4 shows the characteristic peaks of silicon dioxide at 3852.3, 3169.1, 2554.2, 1993.8 and 1495.6 cm^{-1} corresponding to O-H, N-H single bond stretch, C-H single bond stretch, nitriles and carbenes triple bond, C=O, C=C double bond and C-O, C-C single bond respectively. According to Saravanan and Dubey (2020), the spectrum of SiO_2 showed characteristic peaks at 3700 cm^{-1} indicating the presence of –OH stretching bond. The strong bonds at 1093, 459 and 798 cm^{-1} were associated to the asymmetric and symmetric Si-O—Si stretching vibration bonding.

Figure 5 shows the characteristic peaks of starch at 3675.0, 3269.4, 2434.3, 1900.5 and 1428.8 corresponding to –O-H, single bond stretch, C-H single bond stretch, nitriles and carbenes triple bond, C=O C=C double bond, C-O, C-C single bond respectively. According to Abdullah *et al.* (2018) the spectrum of starch showed characteristics peaks at 3448 for –OH stretching, 2930 for –CH stretching, 1646 for C-O bending associated with OH group, and 1381 cm^{-1} associated with –CH symmetric bending.

Figure 6 shows the characteristic peaks of magnesium stearate at 3900.1, 3143.6, 2427.5, 1873.9 and 1454.0 cm^{-1} corresponding to –OH, -NH single bond stretch, -CH single bond stretch, C=O, C=C and C-O, C-C single bond respectively. According to Sue *et al.* (2006), the twin peaks at 1577 and 1466 cm^{-1} were attributed to asymmetric carbohydrate (-COO) stretching vibration and symmetric carbohydrate vibration respectively, while peaks at 2917 and 2850 cm^{-1} were attributed to the –CH stretching vibration.

Figure 7 shows the characteristic peaks of celecoxib + MCC + starch + magnesium stearate + SiO_2. When compared with the pure drug, there was no characteristic change in the above peaks, thus there was no incompatibility with the excipients utilized in the formulation of liquisolid compacts.

Figure 8 shows the characteristic peaks of Tween 80, a non-volatile solvent at 3802.8, 2934.6, 2385.6, 2085.6, 2088.5 and 1392.1 cm^{-1} corresponding to –OH single bond stretch, -CH single bond stretch, carbenes, C=C, C=O double bond and C-C, C-O single bond respectively. According to the FTIR spectrum of Tween 80 showed asymmetric and symmetric stretching bands of (-CH_2) at 2907 and 2855 cm^{-1} respectively, a stretching band at 1735 cm^{-1} due to the C=O ester group and a strong band at 3436 cm^{-1} associated with the hydroxyl stretching vibrations.

Figure 9 shows the characteristic peaks of PEG 400 at 3865.2, 2503.5, 1990.5 and 1422.1 cm^{-1} corresponding to –OH single bond stretch, -CH single bond stretch, C=C and C-C double and single bonds respectively.

Figure 10 shows the characteristic peaks of lactose at 3864.4, 3263.7, 1949.6 and 1121.9 cm^{-1} corresponding to -OH single bond stretch, -CH single bond stretch, C=C and C-C double and single bond respectively.

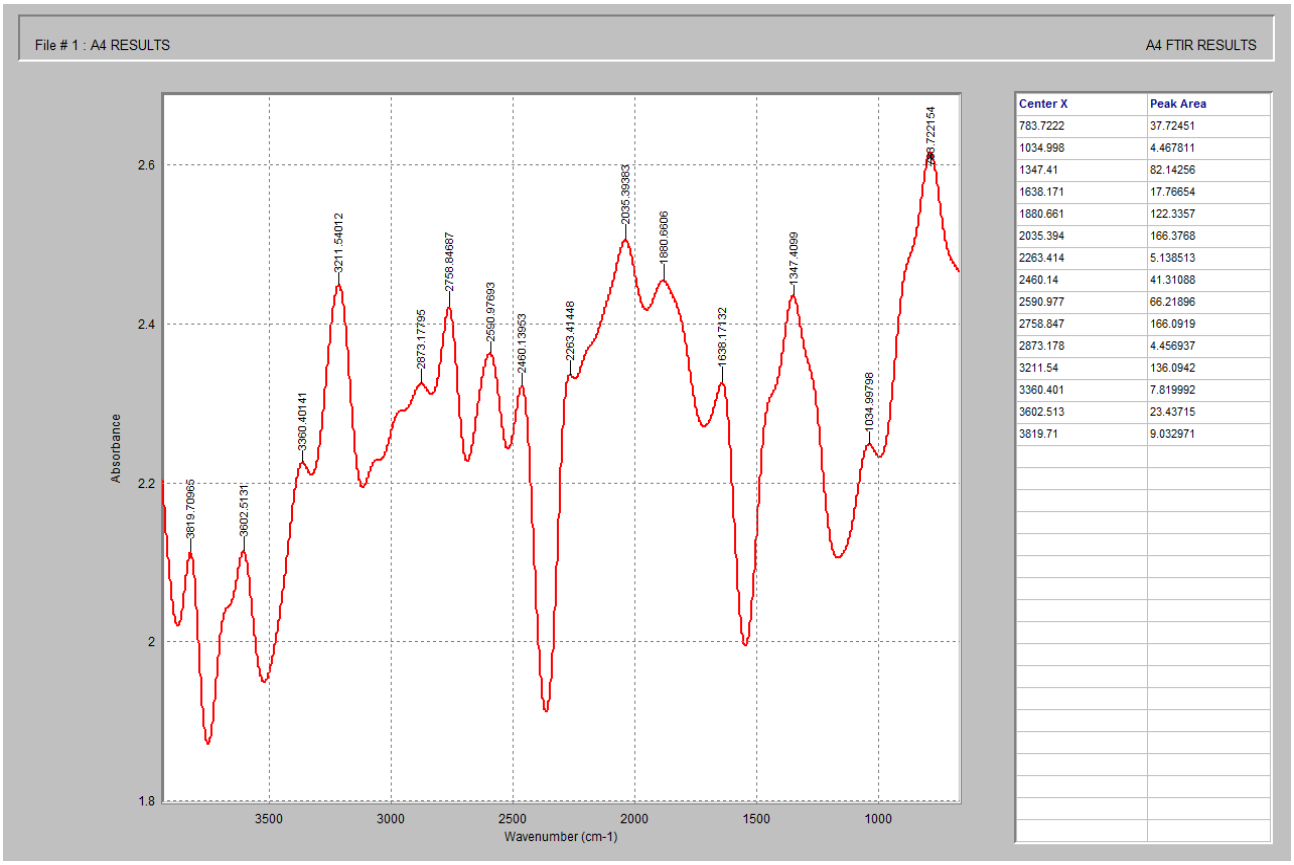

Center X	Peak Area
783.7222	37.72451
1034.998	4.467811
1347.41	82.14256
1638.171	17.76654
1880.661	122.3357
2035.394	166.3768
2263.414	5.138513
2460.14	41.31088
2590.977	66.21896
2758.847	166.0919
2873.178	4.456937
3211.54	136.0942
3360.401	7.819992
3602.513	23.43715
3819.71	9.032971

Figure 2: FTIR spectrum of Celecoxib

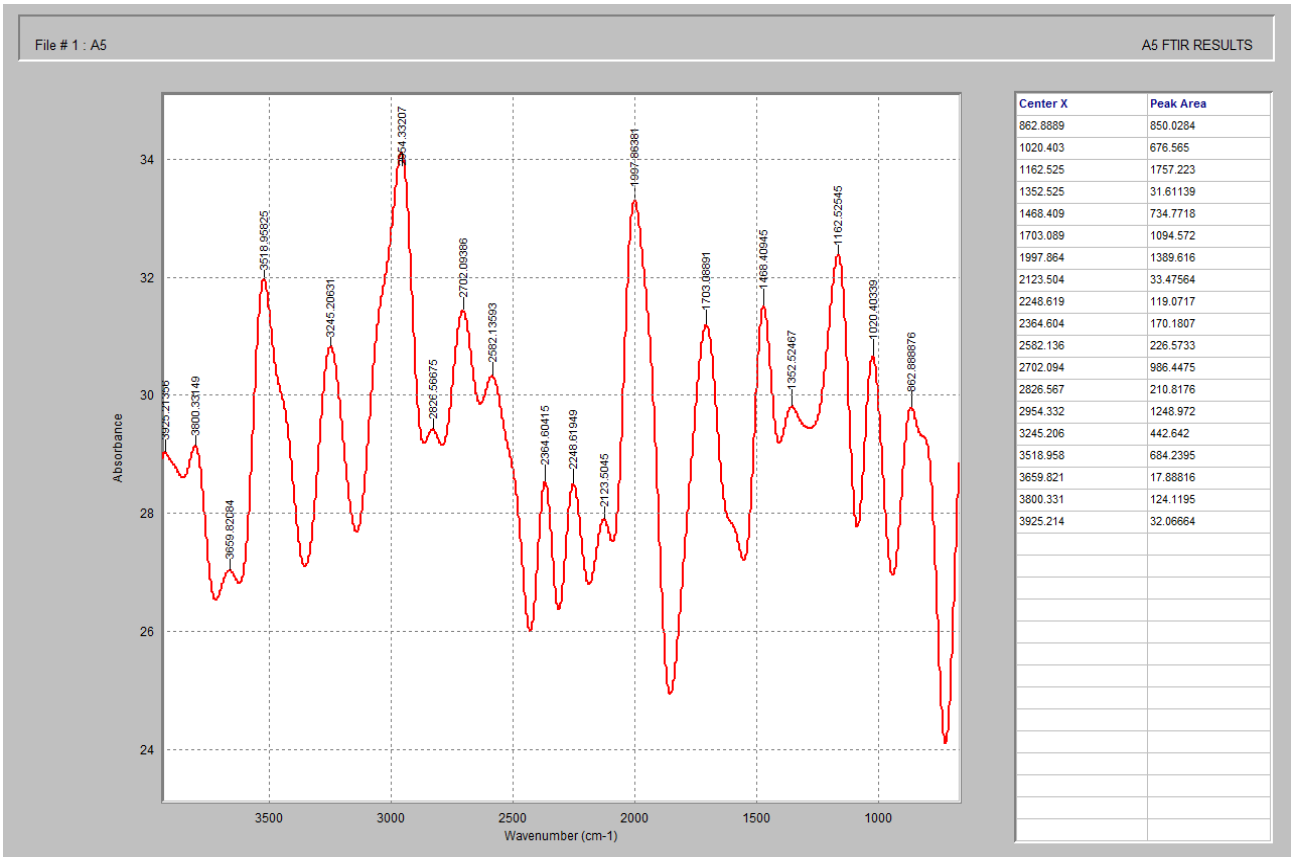

Center X	Peak Area
862.8889	850.0284
1020.403	676.565
1162.525	1757.223
1352.525	31.61139
1468.409	734.7718
1703.089	1094.572
1997.864	1389.616
2123.504	33.47564
2248.619	119.0717
2364.604	170.1807
2582.136	226.5733
2702.094	986.4475
2826.567	210.8176
2954.332	1248.972
3245.206	442.642
3518.958	684.2395
3659.821	17.88816
3800.331	124.1195
3925.214	32.06664

Figure 3: FTIR of microcrystalline cellulose

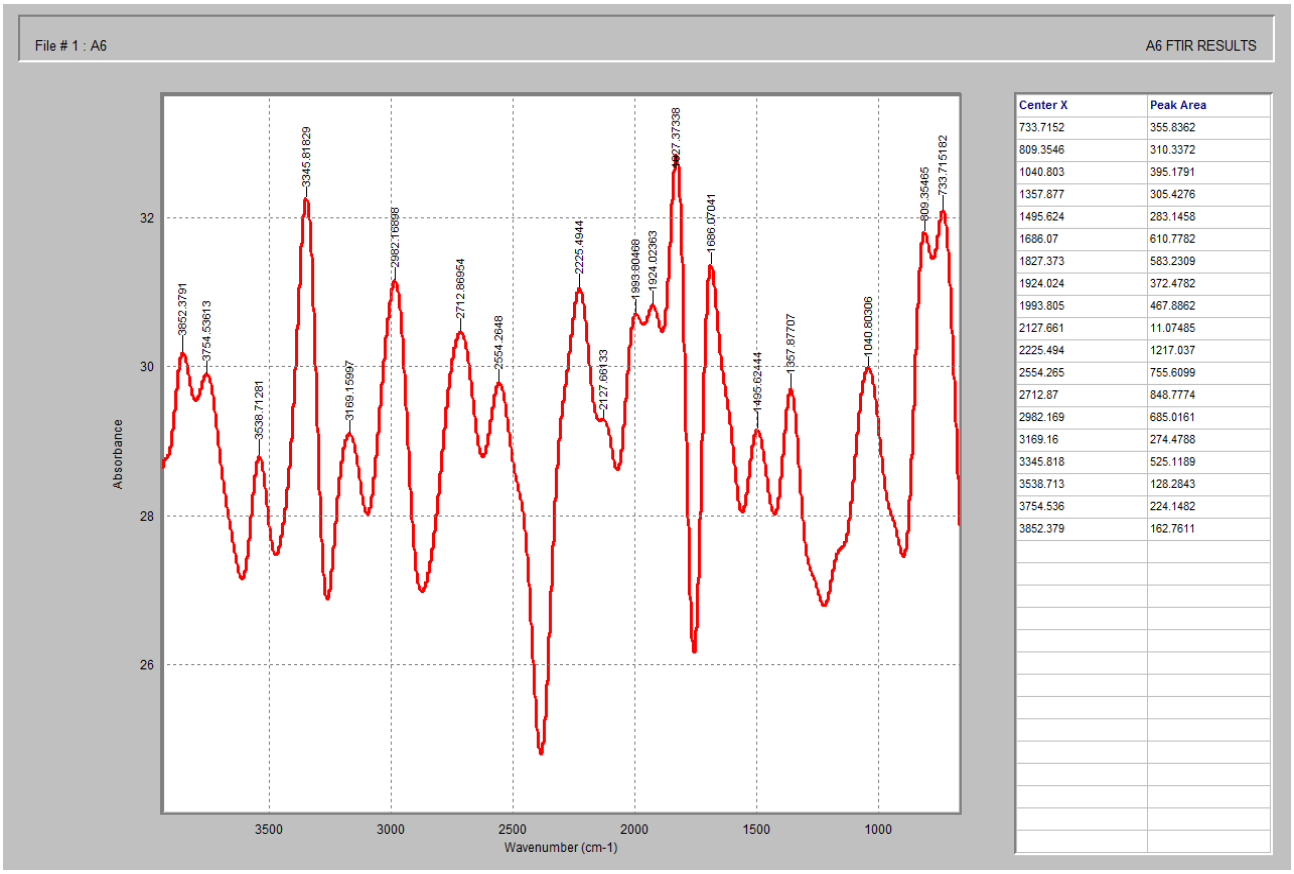

Center X	Peak Area
733.7152	355.8362
809.3546	310.3372
1040.803	395.1791
1357.877	305.4276
1495.624	283.1458
1686.07	610.7782
1827.373	583.2309
1924.024	372.4782
1993.805	467.8862
2127.661	11.07485
2225.494	1217.037
2554.265	755.6099
2712.87	848.7774
2982.169	685.0161
3169.16	274.4788
3345.818	525.1189
3538.713	128.2843
3754.536	224.1482
3852.379	162.7611

Figure 4: FTIR spectrum of silicon dioxide

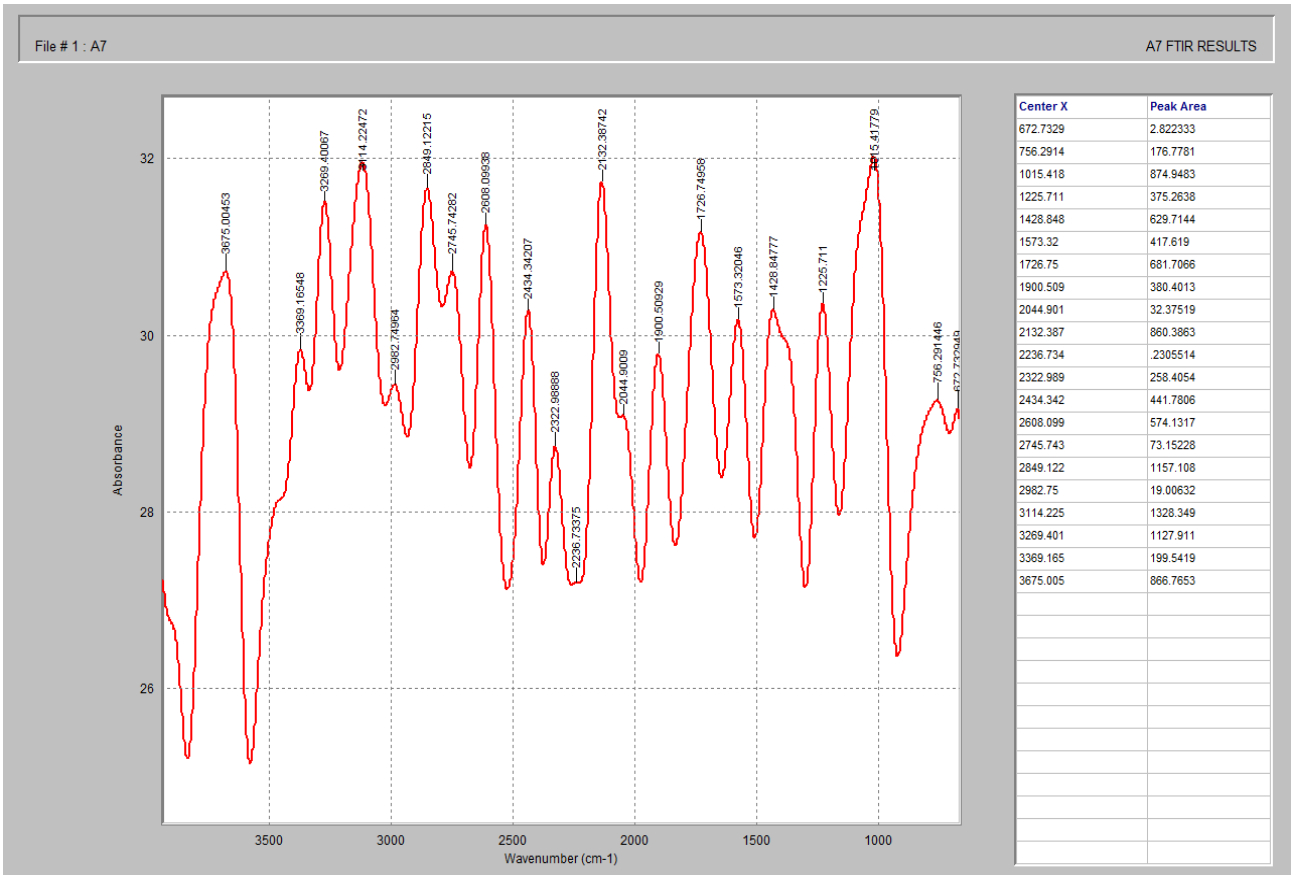

Center X	Peak Area
672.7329	2.822333
756.2914	176.7781
1015.418	874.9483
1225.711	375.2638
1428.848	629.7144
1573.32	417.619
1726.75	681.7066
1900.509	380.4013
2044.901	32.37519
2132.387	860.3863
2236.734	.2305514
2322.989	258.4054
2434.342	441.7806
2608.099	574.1317
2745.743	73.15228
2849.122	1157.108
2982.75	19.00632
3114.225	1328.349
3269.401	1127.911
3369.165	199.5419
3675.005	866.7653

Figure 5: FTIR spectrum of starch

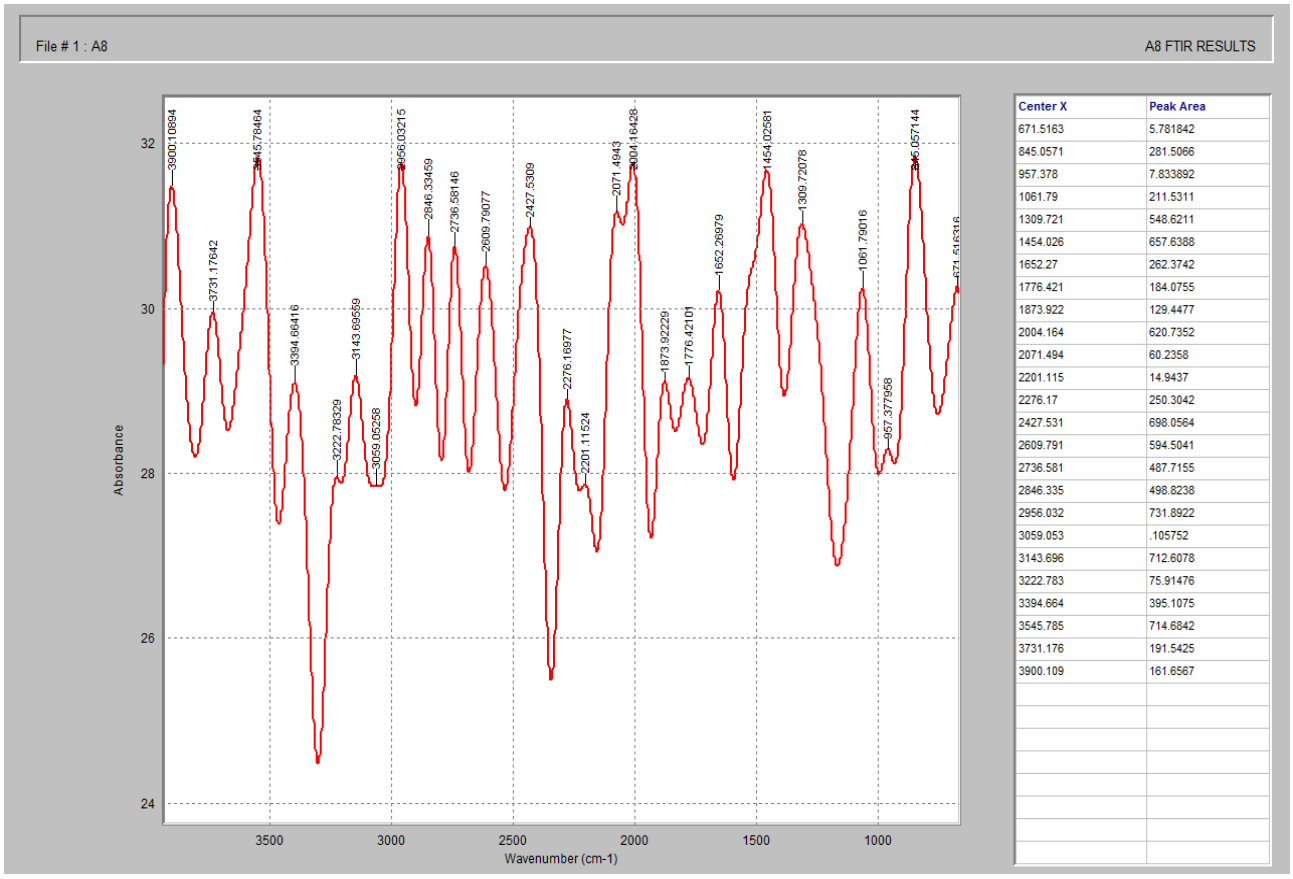

Figure 6: FTIR spectrum of magnesium stearate

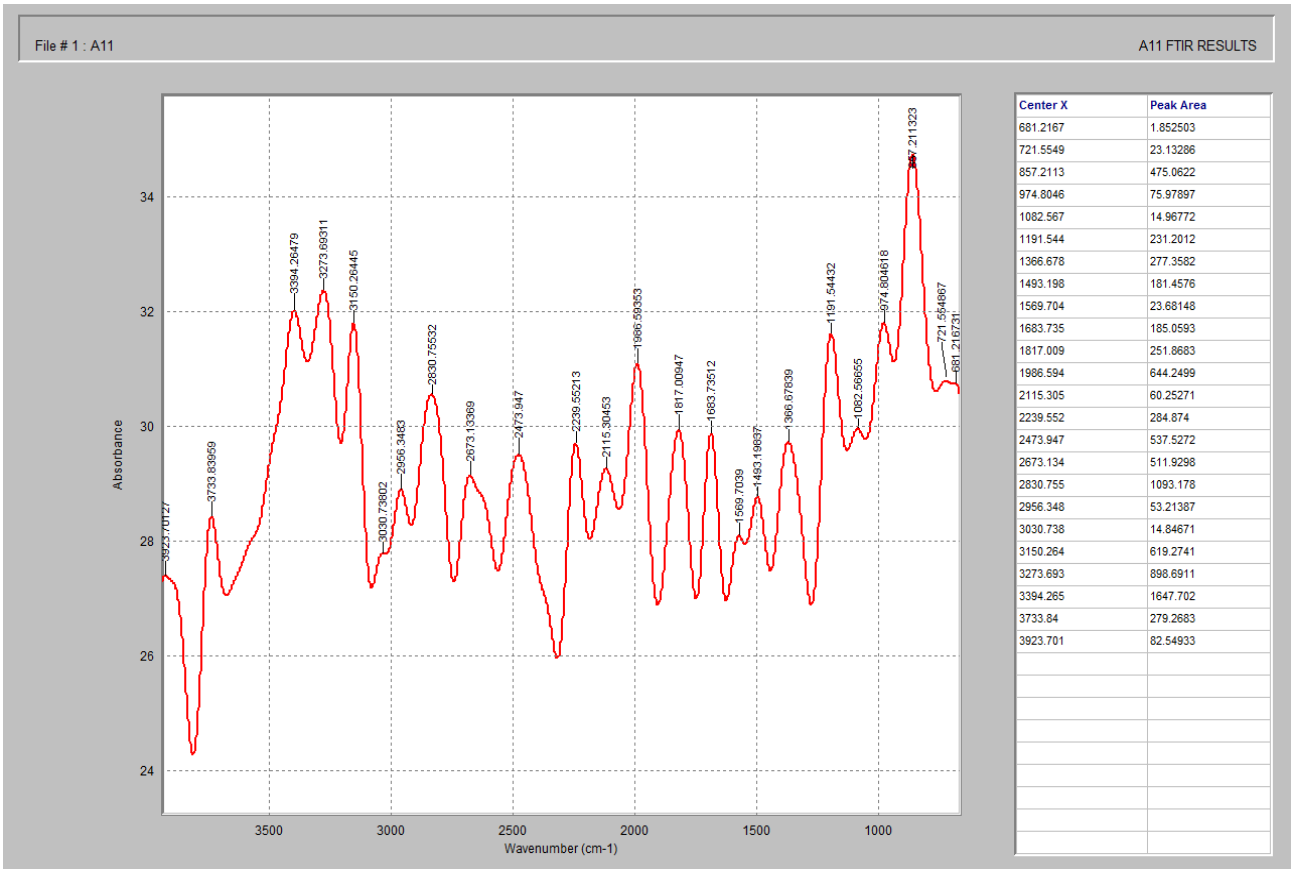

Figure 7: FTIR spectrum of celecoxib + MCC + starch + magnesium stearate + silicon dioxide

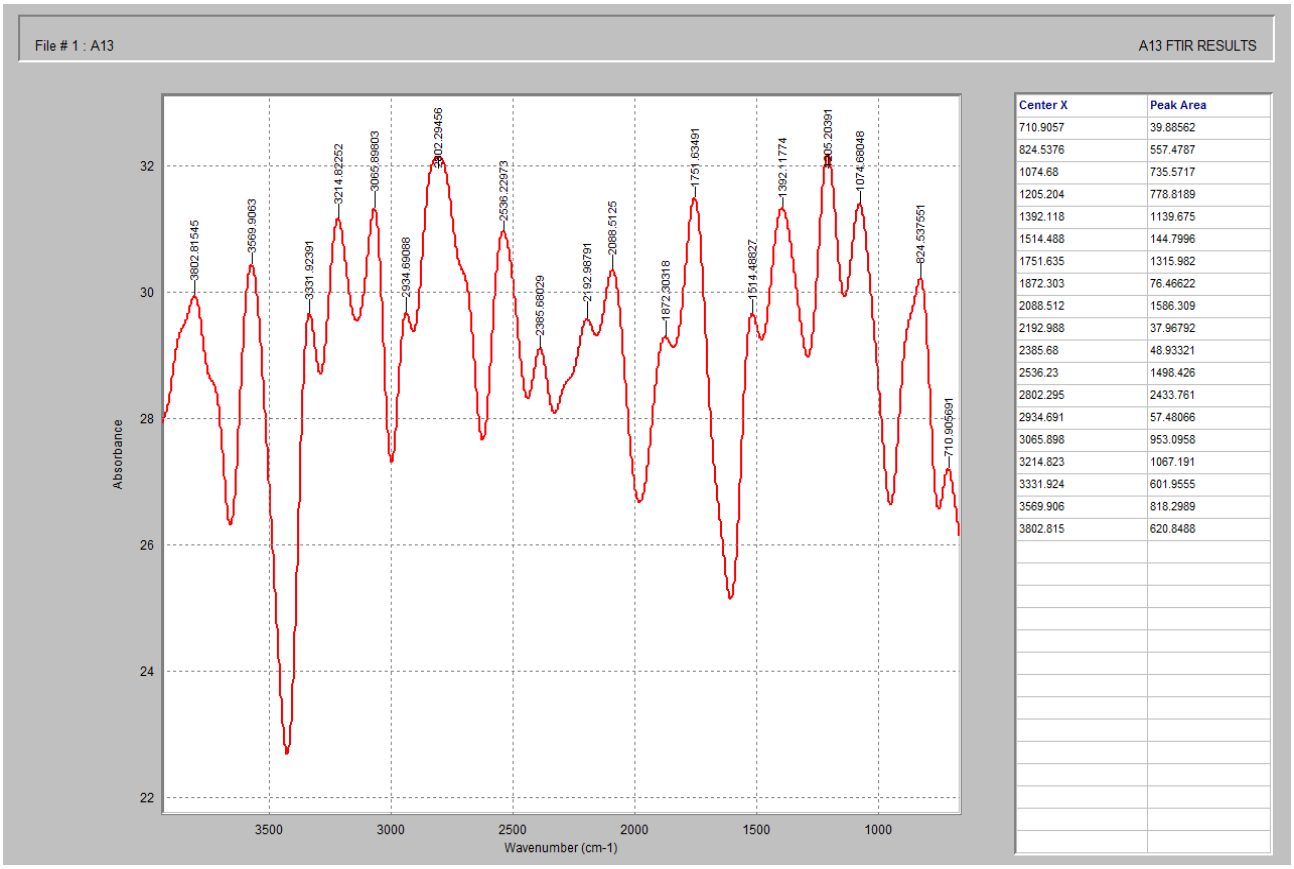

Center X	Peak Area
710.9057	39.88562
824.5376	557.4787
1074.68	735.5717
1205.204	778.8189
1392.118	1139.675
1514.488	144.7996
1751.635	1315.982
1872.303	76.46622
2088.512	1586.309
2192.988	37.96792
2385.68	48.93321
2536.23	1498.426
2802.295	2433.761
2934.691	57.48066
3065.898	953.0958
3214.823	1067.191
3331.924	601.9555
3569.906	818.2989
3802.815	620.8488

Figure 8: FTIR spectrum of Tween 80

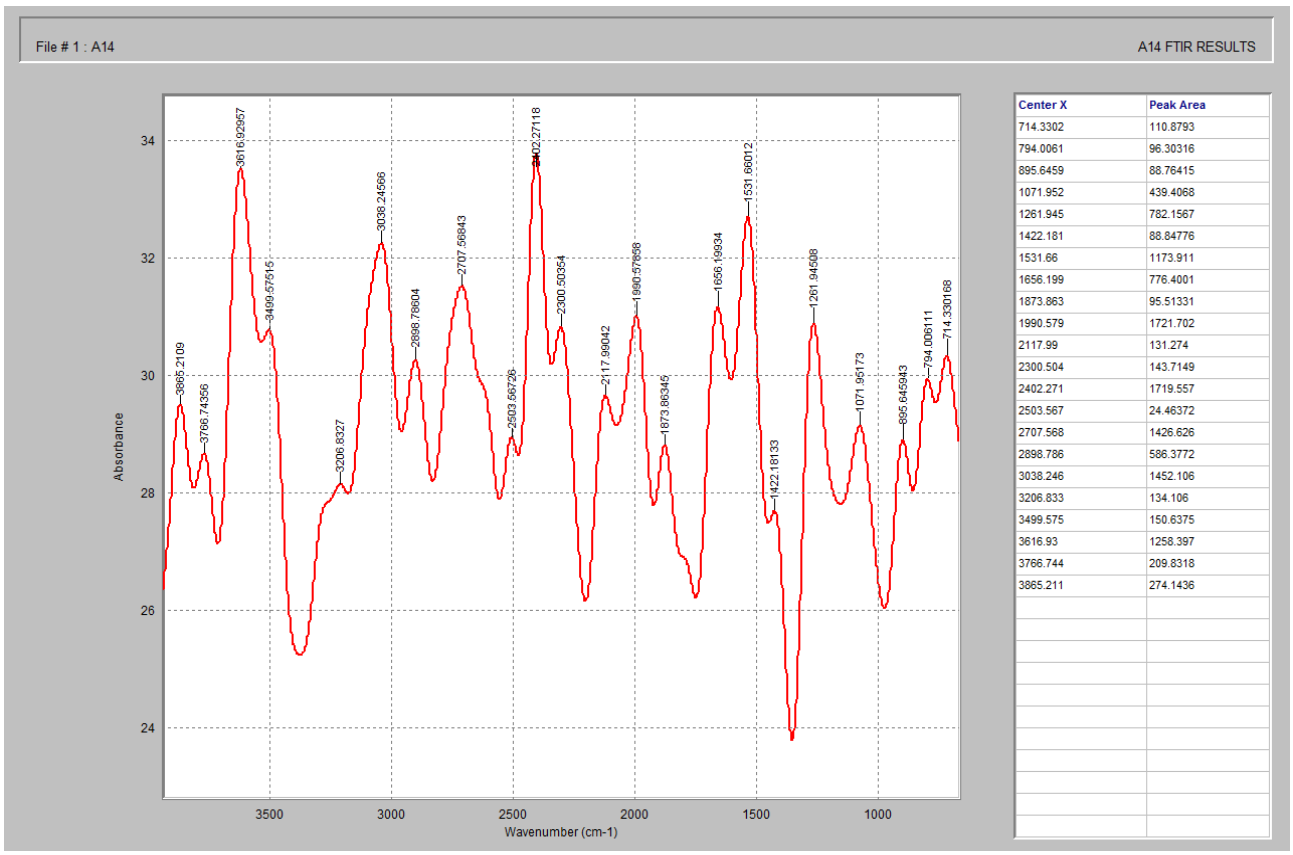

Center X	Peak Area
714.3302	110.8793
794.0061	96.30316
895.6459	88.76415
1071.952	439.4068
1261.945	782.1567
1422.181	88.84776
1531.66	1173.911
1656.199	776.4001
1873.863	95.51331
1990.579	1721.702
2117.99	131.274
2300.504	143.7149
2402.271	1719.557
2503.567	24.46372
2707.568	1426.626
2898.786	586.3772
3038.246	1452.106
3206.833	134.106
3499.575	150.6375
3616.93	1258.397
3766.744	209.8318
3865.211	274.1436

Figure 9: FTIR spectrum of PEG 4000

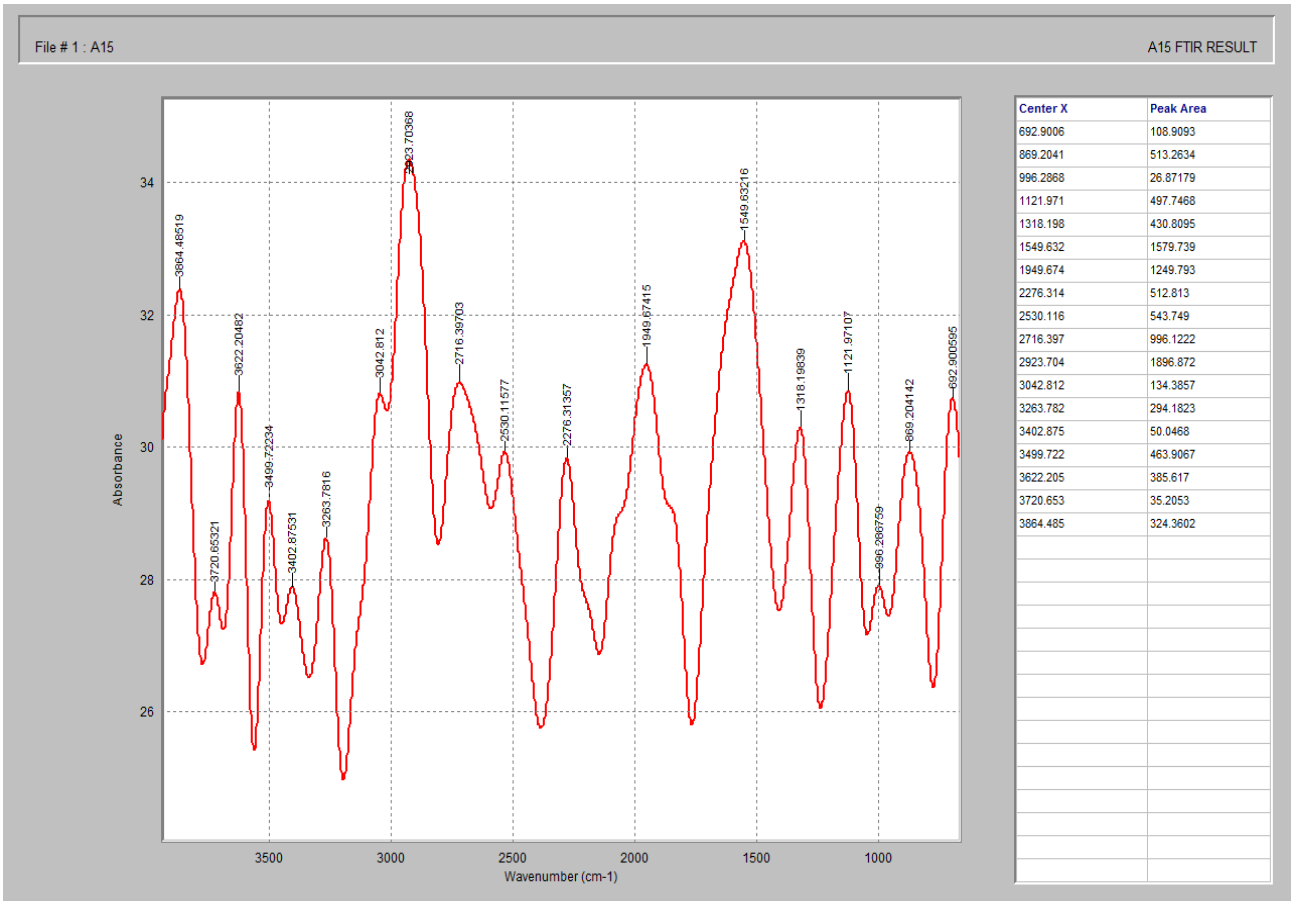

Center X	Peak Area
692.9006	108.9093
869.2041	513.2634
996.2868	26.87179
1121.971	497.7468
1318.198	430.8095
1549.632	1579.739
1949.674	1249.793
2276.314	512.813
2530.116	543.749
2716.397	996.1222
2923.704	1896.872
3042.812	134.3857
3263.782	294.1823
3402.875	50.0468
3499.722	463.9067
3622.205	385.617
3720.653	35.2053
3864.485	324.3602

Figure 10: FTIR spectrum of lactose

Evaluation of Liquisolid Granules and Conventional Tablet

Angle of Repose

The angle of repose is a characteristic of the internal function or cohesion of the particles. If a powder is non-cohesive, the angle of repose will be high, but if a powder is cohesive, the angle of repose will be low (ASTM International, 2014).

For the celecoxib liquisolid granules, the angle of repose for the pure drug was 27.22 ± 0.05, while that of the conventional tablet was 24.32 ± 0.38. The formulation with the extracted and reference lecithin recorded 0.23 ± 0.01 and 0.25 ± 0.03 respectively. The lowest angle of repose was recorded in F-EL, while the highest was recorded in F-5 (27.75 ± 1.09).

Bulk Density

Bulk density was used to measure the flow properties of the powder. It is a function of the particle size and particle size distribution. It has a direct relationship with the flow characteristics of a powder. For celecoxib, the angle of repose of the pure drug was 27.22 ± 0.05, while that of the CT was 24.32 ± 0.38. The formulation with the extracted and reference lecithin recorded 0.23 ± 0.01 and 0.25 ± 0.03 respectively. The lowest value was recorded in F-EL (23.90 ± 0.11), while the highest value was recorded in F-5 (27.75 ± 1.09).

Tapped Density

Tapped density is a function of particle size and size distribution. For celecoxib powder blend, the pure drug was 0.30 ± 0.01, while that of the conventional tablet was 0.34 ± 0.01. The formulation with extracted and reference lecithin recorded 0.29 ± 0.02 and 0.32 ± 0.01 respectively.

Carr's Index (Compressibility Index)

This is affected by particle size and particle size distribution. According to BP specifications, excellent free flowing granules range from 5-15%, while good free flowing granules range from 12-16%. Very poor fluid cohesive powders have C.I of > 38%, while powders with C.I. > 40% indicates very poor flow.

Hausner's Ratio (HR)

It has a direct relationship between he tapped and bulk density. According to specifications, excellent free flowing granules range from 1.00 ± 1.11, while good free flowing granules range from 1.12 to 1.18. Very poor fluid cohesive powders have H.R. of 1.6 to 1.59. For

celecoxib, the pure drug was 1.15 ± 0.01, while that of the conventional tablet was 1.27 ± 0.04. The extracted and reference lecithin recorded 16.05 ± 0.60 and 16.90 ± 0.70 respectively.

Drug Content

The drug content was used to determine the uniform amount of pharmaceutical active ingredients that were present in all the formulations. Celecoxib powder blend, indicated that the drug content was within the range of 95.4 ± 0.65 to 99.0 ± 1.07. They were within the acceptable range as specified in the Indian Pharmacopoeia.

Table 3: Evaluation of pre-compression parameters of liquisolid granules of Celecoxib (n =3, all values are written as Mean ± SD)

Pure drug/codes	Angle of repose (^{o})	Bulk density (g/ml)	Tapped density (g/ml)	Hausners Ratio	Compressibility index (%)
Celecoxib	27.22 ± 0.05	0.23 ± 0.01	0.30 ± 0.01	1.15 ± 0.01	21.32 ± 2.89
F-1	26.52 ± 0.79	0.24 ± 0.01	0.34 ± 0.03	1.17 ± 0.01	20.08 ± 2.11
F-2	24.12 ± 1.21	0.25 ± 0.01	0.25 ± 0.01	1.14 ± 0.02	20.51 ± 1.47
F-3	24.75 ± 1.44	0.25 ± 0.01	0.29 ± 0.01	1.18 ± 0.01	19.92 ± 1.83
F-4	25.85 ± 0.38	0.25 ± 0.01	0.26 ± 0.01	1.23 ± 0.01	19.82 ± 1.75
F-5	27.75 ± 1.09	0.23 ± 0.01	0.29 ± 0.01	1.17 ± 0.01	20.92 ± 0.41
F-6	24.92 ± 0.93	0.24 ± 0.01	0.34 ± 0.01	1.18 ± 0.03	19.31 ± 1.48
F-7	25.95 ± 0.45	0.23 ± 0.01	0.31 ± 0.01	1.18 ± 0.02	19.52 ± 0.76
F-8	25.72 ± 0.22	0.25 ± 0.01	0.28 ± 0.01	1.25 ± 0.01	19.96 ± 0.38
F-9	25.87 ± 1.25	0.25 ± 0.01	0.27 ± 0.01	1.26 ± 0.02	17.86 ± 1.01
F-10	24.57 ± 1.18	0.28 ± 0.02	0.27 ± 0.01	1.24 ± 0.01	19.79 ± 0.45
F-11	24.82 ± 0.44	0.27 ± 0.01	0.30 ± 0.01	1.24 ± 0.01	22.42 ± 2.72
F-12	26.72 ± 0.93	0.30 ± 0.01	0.35 ± 0.01	1.13 ± 0.01	14.04 ± 0.94
CT	24.32 ± 0.38	0.24 ± 0.01	0.34 ± 0.01	1.27 ± 0.04	18.00 ± 0.36

Carrier materials: F-1 to F-4, CT, lactose; F-5 to F-8: Sorbitol
Coating materials: F1-F6: Silicon dioxide (SiO_2); F7-F12, CT : Talc.
Disintegrants: F1-F6, CT: Maize starch; F7-F12: Sodium starch glycolate.
F-9 to F-12: MCC. CT: Conventional tablet (without non-volatile solvent)

Table 4: Drug content of Celecoxib powder blend (n =3, all values are written as Mean ± SD)

Formulation code	Celecoxib
F-1	97.1 ± 1.59
F-2	97.4 ± 0.07
F-3	96.9 ± 0.38
F-4	97.0 ± 0.15
F-5	96.7 ± 0.42
F-6	95.9 ± 0.65
F-7	96.3 ± 0.31
F-8	95.4 ± 0.65
F-9	96.9 ± 0.58
F-10	95.9 ± 0.40
F-11	96.1 ± 0.90
F-12	95.7 ± 0.74
CT	95.7 ± 0.98

Carrier materials: F-1 to F-4, CT: lactose; F-5 to F-8: Sorbitol
Coating materials: F1-F6: Silicon dioxide (SiO_2); F7-F12, CT: Talc.
Disintegrants: F1-F6, CT: Maize starch; F7-F12: Sodium starch glycolate.
F-9 to F-12: MCC. CT: Conventional tablet (without non-volatile solvent)

Post Compressional Evaluation of liquisolid Tablets

For each drug, the different formulations were evaluated for the post compressional parameters such as general appearance, uniformity of weight, hardness, friability, disintegration time and thickness and diameter.

General Appearance of Tablets

The formulated liquisolid tablets were white in colour, with both standard capsule and round shape. All the liquisolid tablets were elegant in appearance.

Tablet Thickness

For celecoxib, the thickness values were found in the range of 3.80 ± 0.21 for batch F-RL to 4.90 ± 0.00 for batch F-3 respectively. Mechanical wear and imperfections in the pressing or tooling may also introduce variability which can cause buildup of materials on the punch face and the die wall. These factors may subsequently affect tablet weight and the physical consistency of manufactured tablets.

Friability

Tablets are always subjected to mechanical shocks during handling, packaging and transportation. When this happens, the stress on the tablets could lead to chipping, breaking or capping. Other factors that could affect tablet strength include the poor tablet design, low moisture content, insufficient binder and over lubrication. Friability of a tablet is determined using the Roche friabilator. It consists of a plastic chamber that revolves at 25 rpm dropping the tablets through a distance of six inches in the friabilator which is operated for 100 revolutions. Acceptable range for tablet friability is 0.5 to 1% (Blagden *et al.*, 2007). Celecoxib recorded a friability range was 0.40 ± 0.00 for reference commercial tablet and 0.66 ± 0.01 for batch F-3. They were within the acceptable limit for friability.

Disintegration

The disintegration time of all the tablet formulations were determined using the disintegration test apparatus. The disintegration test is used to show how quickly the tablet breaks down into smaller particles thereby allowing for a greater surface area and availability of the drug.

Celecoxib recorded a disintegration time of 2.25 ± 0.35 for batch F-EL and 12.40 ± 0.21 for batch reference commercial tablet. They were within the acceptable limits for uncoated tablets.

Weight Variation

The weight variation was used to determine the uniformity of the tablets in all formulations. The result obtained, showed that all the formulated tablets passed the weight variations within the acceptable limit as per Indian Pharmacopoeia (none of the formulated tablets weight differed from the mean by more than 10%). According to BP 1988 specification for uncoated tablets, the mean weight for 20 tablets recorded, the tablets weighing 80 mg or less should not deviate by more than 10%, while for tablets weighing between 80-250 mg should not deviate by more than 7.5%. For tablets weighing 250 m g or more, the deviation should not be more than 5%.

Table 5: Post-compressional evaluation of liquisolid tablets of Celecoxib (n =3, all values are written as Mean ± SD)

Formulation code	General appearance	Hardness (kg/cm^2)	Thickness (mm)	Diameter (mm)	Weight variation (mg)	Friability (%)	Disintegration time (sec)
F-1	White	5.15 ± 0.74	4.50 ± 0.28	5.31 ± 0.20	666.4 ± 3.95	0.61 ± 0.07	4.65 ± 0.10
F-2	White	4.90 ± 0.56	4.60 ± 0.21	5.15 ± 0.29	677.4 ± 1.62	0.59 ± 0.08	5.45 ± 0.17
F-3	White	4.60 ± 0.35	4.90 ± 0.00	4.95 ± 0.10	686.0 ± 2.86	0.66 ± 0.01	4.25 ± 0.10
F-4	White	4.55 ± 0.31	4.45 ± 0.24	4.80 ± 0.07	750.8 ± 2.68	0.47 ± 0.12	5.50 ± 0.28
F-5	White	4.55 ± 0.24	4.75 ± 0.03	4.96 ± 0.04	766.6 ± 1.83	0.55 ± 0.03	5.75 ± 0.24
F-6	White	4.50 ± 0.24	4.50 ± 0.14	4.46 ± 0.30	783.4 ± 0.31	0.55 ± 0.03	4.70 ± 0.14
F-7	White	4.55 ± 0.24	4.40 ± 0.21	4.50 ± 0.21	759.9 ± 0.63	0.62 ± 0.01	5.50 ± 0.28
F-8	White	4.65 ± 0.03	4.30 ± 0.28	4.60 ± 0.14	771.7 ± 2.61	0.60 ± 0.00	6.90 ± 0.21
F-9	White	4.75 ± 0.03	4.35 ± 0.17	4.95 ± 0.10	786.5 ± 2.51	0.61 ± 0.01	6.90 ± 0.14
F-10	White	4.70 ± 0.07	4.20 ± 0.21	4.80 ± 0.16	848.7 ± 4.03	0.59 ± 0.01	5.10 ± 0.07
F-11	White	4.70 ± 0.14	4.30 ± 0.07	4.72 ± 0.24	863.9 ± 3.46	0.45 ± 0.03	5.50 ± 0.28
F-12	White	4.70 ± 0.14	4.20 ± 0.07	4.55 ± 0.24	883.6 ± 0.28	0.50 ± 0.00	5.75 ± 0.10
CT	White	4.50 ± 0.21	4.50 ± 0.21	4.45 ± 0.17	606.9 ± 2.75	0.50 ± 0.00	13.30 ± 0.14
RCT	White	3.85 ± 0.60	3.85 ± 0.60	4.56 ± 0.32	4.00 ± 2.80	0.40 ± 0.00	12.40 ± 0.21

Carrier materials: F-1 to F-4, CT: lactose; F-5 to F-8: Sorbitol

Coating materials: F1-F6: Silicon dioxide (SiO_2); F7-F12, CT: Talc.

Disintegrants: F1-F6, CT: Maize starch; F7-F12: Sodium starch glycolate.

F-9 to F-12: MCC. CT: Conventional tablet (without non-volatile solvent)

In vitro Release Studies of Liquisolid Formulations and Reference Commercial Tablet

In vitro dissolution studies were carried out by USP type II method by using 0.1 N HCl as the dissolution medium. The studies were performed in all the formulations for 1 hour. The samples were taken at 5 minutes interval for first 30 minutes and 15 minutes interval for next 30 minutes and absorbance was measured in UV spectrophotometer at 252 nm. Two formulation parameters that normally affect the drug dissolution rate in immediate release liquisolid tablets were investigated. They include the effect of drug concentration in the liquid medication (ratio of drug and liquid vehicle) and effect of carrier/coating ratio (R-value). The results of the in vitro release studies of celecoxib from liquisolid formulation is shown in Table 6.

For celecoxib formulations, F-1, F-2, F-3, F-4, F-5 and F-6 formulated with lactose and sorbitol (F-5 and F-6) as carrier materials, silicon dioxide as a coating material and maize starch as a disintegrant recorded a release of 84.30 ± 0.00%, 86.60 ± 1.20%, 82.25 ± 1.44%, 81.55 ± 0.95%, 83.35 ± 0.17% and 83.90 ± 0.56% respectively, while formulations F-7, F-8, F-9, F-10, F-11 and F-12 formulated with talc as a coating material and sodium starch glycolate as a disintegrant recorded release at 81.65 ± 1.02, 83.30 ± 0.42%, 85.35 ± 0.74%, 82.25 ± 0.31%, 83.70 ± 0.42% and 84.40 ± 0.91% respectively. The conventional tablet (without the non-volatile solvent) recorded 77.45 ± 0.74%. According to Nafiseh *et al*, (2022), the wettability of the liquisolid formulation is improved due to the presence of hydrophilic liquid vehicle, therefore more of the drug particles is exposed to the dissolution medium which subsequently leads to improved dissolution rate (Nafiseh *et al.*, 2022). The dissolution rate of drugs in the dissolution medium depends on the contact area of the drug with the dissolution medium. At a constant rotational speed of the paddle at 50 rpm in combination with the dissolution medium, the thickness of the static diffusion layer and the diffusion coefficient of the drug molecules can be considered the same. According to Noye-Whitneys equation, increased solubility occurs with a decrease in drug particle size.

Table 6: In-vitro release profile of Celecoxib liquisolid formulations

Time (min)	Dissolution medium	F-1	F-2	F-3	F-4	F-5	F-6	F-7	F-8	F-9	F-10	F-11	F-12	F-CT	RCT
0	0.1 N HCl	0	0	0	0	0	0	0	0	0	0	0	0	0	0
5		35.15 ± 0.24	33.90 ± 0.56	31.95 ± 2.01	29.58 ± 0.33	34.20 ± 0.63	33.91 ± 0.83	32.10 ± 2.12	32.45 ± 0.74	35.10 ± 0.28	33.00 ± 0.35	35.30 ± 0.14	34.10 ± 0.70	36.1 ± 0.24	24.90 ± 0.21
10		48.85 ± 0.45	42.50 ± 1.69	41.85 ± 2.36	39.35 ± 0.60	41.25 ± 0.95	41.31 ± 0.99	39.20 ± 0.49	41.85 ± 0.53	45.70 ± 0.56	40.54 ± 0.39	43.20 ± 2.33	40.00 ± 0.70	46.85 ± 0.24	36.30 ± 0.28
15		56.65 ± 0.31	53.00 ± 0.07	53.59 ± 2.47	54.24 ± 2.93	52.20 ± 0.07	52.53 ± 0.16	51.19 ± 0.78	54.10 ± 0.91	54.65 ± 1.09	52.35 ± 0.31	54.25 ± 1.37	52.60 ± 0.21	50.00 ± 0.00	45.05 ± 0.24
20	0.1 N HCl	63.80 ± 0.63	61.40 ± 0.63	60.40 ± 2.19	58.25 ± 0.67	57.25 ± 1.52	60.02 ± 0.44	58.35 ± 0.74	59.90 ± 0.28	63.20 ± 0.63	59.20 ± 0.21	61.75 ± 1.66	59.95 ± 0.38	56.95 ± 0.88	48.85 ± 0.03
25		69.80 ± 0.21	68.80 ± 0.28	64.50 ± 2.54	62.30 ± 0.98	61.50 ± 0.91	64.66 ± 1.31	61.85 ± 0.67	65.05 ± 1.16	69.55 ± 0.24	62.72 ± 0.47	66.35 ± 2.51	65.60 ± 1.97	65.30 ± 0.14	54.80 ± 0.21
30		74.70 ± 0.42	75.00 ± 0.21	69.90 ± 2.96	65.90 ± 0.14	68.45 ± 1.16	71.01 ± 0.64	67.90 ± 1.55	70.00 ± 0.42	75.30 ± 0.00	69.65 ± 0.17	72.70 ± 1.83	72.40 ± 1.62	70.50 ± 0.14	58.85 ± 0.74
45	0.1 N HCl	80.15 ± 0.03	82.50 ± 0.14	75.05 ± 3.57	72.60 ± 1.83	73.25 ± 0.24	76.27 ± 1.89	71.80 ± 1.27	75.80 ± 2.61	81.25 ± 0.74	72.25 ± 0.10	76.90 ± 2.33	78.15 ± 3.21	72.80 ± 0.49	63.90 ± 0.21
60		84.30 ± 0.00	86.60 ± 1.20	82.25 ± 1.44	81.55 ± 0.95	83.35 ± 0.17	83.90 ± 0.56	81.65 ± 1.02	83.30 ± 0.42	85.35 ± 0.74	82.25 ± 0.31	83.70 ± 0.42	84.40 ± 0.91	77.45 ± 0.74	68.50 ± 0.28

Carrier materials: F-1 to F-4, CT: lactose; F-5 to F-8: Sorbitol

Coating materials: F1-F6: Silicon dioxide (SiO_2); F7-F12, CT: Talc.

Disintegrants: F1-F6, CT: Maize starch; F7-F12: Sodium starch glycolate.

F-9 to F-12: MCC. CT: Conventional tablet (without non-volatile solvent)

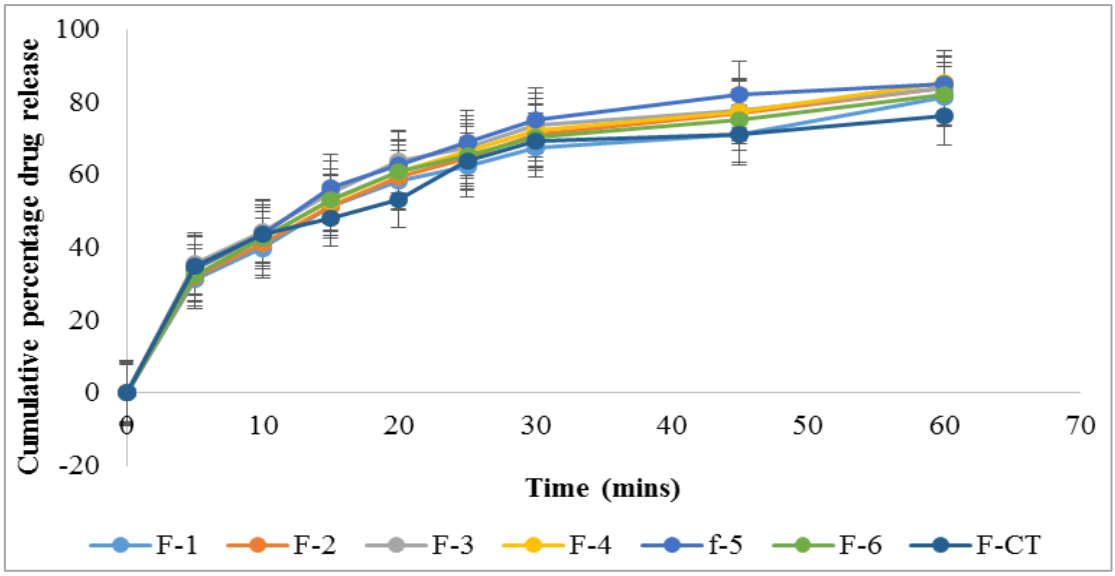

Figure 11: Drug release profile of batches F1 to F-6 and F-CT in 0.1 N HCl

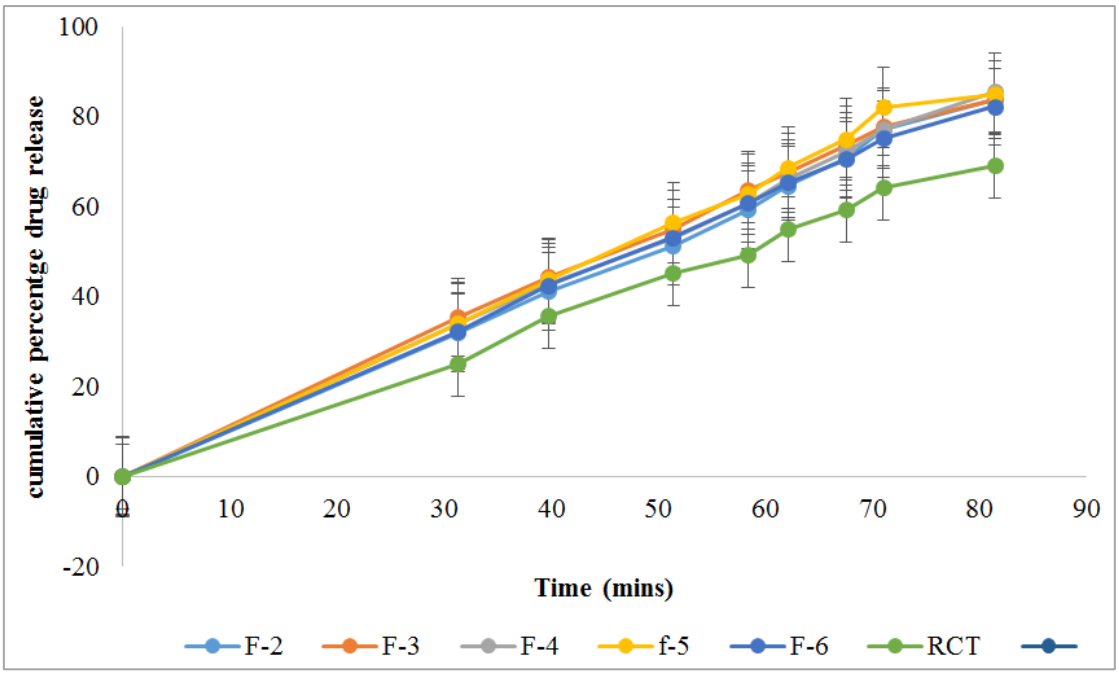

Figure 12: Drug release profile of batches F1 to F6 and R-CT in 0.1 N HCl

***In vitro* Drug Release Kinetics of the Liquisolid Tablets**

The *in vitro* drug release kinetics of the various formulations were investigated by using the various important mathematical models such as zero order (cumulative % drug release vs time), first order (log cumulative % drug release vs time), Higuchi matrix (cumulative % drug release vs square root of time), Korsmeyer-Peppas (log cumulative % drug release vs log time) and Hixson-Crowell. The release constants were calculated from the slopes of the respective plots. The release profile was interpreted and evaluated by the correlation coefficient (r^2).

For the zero-order release kinetic model, the batch with the highest r^2 value was batch F-10 with a value of 0.9353, while the lowest r^2 value was recorded in batch F-1 with a value of 0.9153.

For the first order release kinetic model, the batch with the highest r^2 value was 0.9986, was F-1, while the lowest r^2 value was batch RCT with 0.9850.

For the Higuchi kinetic model, the batch with the highest r^2 value was F-CT with 0.9671, while the lowest r^2 value was recorded in batch F-5 with 0.9894.

For Korsmeyer-Peppas model, the formulation batch F-9 had the highest r^2 value of 0.9995 and n-value

of 0.407. According to Korsmeyer-Peppas, when 0.45 < n = 0.89, the release mechanism is non-Fickian transport, while when n > 0.89, the release mechanism is super-case II transport. When n < 0.5, the release mechanism is Fickian transport.

For the Hixson-Crowell, the highest r^2 was recorded in batch F-2, with value of 0.9984, while the lowest r^2 value was recorded in batch R-CT with value of 0.9731.

The liquisolid formulations exhibited best fit for Higuchi equation with r^2 value greater than 0.95. Batch F-2 showed best fit for Hixson-Crowell model which is due to a relatively high drug release rate at initial phase followed by a phase in which the decrease of the release rate was more pronounced. Batch F-9 showed best fit for Korsemeyer-Peppas (0.9995) which is due to drug release by Fickian transport. Batch F-CT showed the highest correlation co-efficient (0.9671) in Higuchi model. It showed that the release of the drug involved both dissolution and diffusion (Baveja *et al.*, 1987). For the zero-order model, batch F-10 showed the highest drug release which is independent of concentration.

Table 7: The Zero order, First order, Higuchi, Korsmeyer- Peppas and Hixson-Crowell models for the drug release of Celecoxib liquisolid formulations

Formulation batch	Zero order	First order	Higuchi	Korsmeyer-Peppas		Hixson-Crowell
	r^2	r^2	r^2	r^2	n	r^2
F-1	0.9153	0.9986	0.9696	0.9962	0.439	0.9970
F-2	0.9336	0.9971	0.9783	0.9893	0.413	0.9984
F-3	0.9274	0.9960	0.9760	0.9918	0.480	0.9913
F-4	0.9295	0.9896	0.9752	0.9852	0.517	0.9832
F-5	0.9578	0.9936	0.9894	0.9883	0.395	0.9933
F-6	0.9413	0.9964	0.9824	0.9785	0.407	0.9950
F-7	0.9400	0.9925	0.9803	0.9869	0.463	0.9886
F-8	0.9338	0.9968	0.9795	0.9934	0.463	0.9932
F-9	0.9232	0.9984	0.9736	0.9995	0.388	0.9984
F-10	0.9353	0.9916	0.9775	0.9890	0.449	0.9944
F-11	0.9301	0.9962	0.9764	0.9826	0.398	0.9944
F-12	0.9373	0.9950	0.9790	0.9786	0.443	0.9948
F-CT	0.9191	0.9950	0.9671	0.9889	0.313	0.9857
RCT	0.9208	0.9850	0.9732	0.9965	0.459	0.9731

*r^2 = Coefficient correlation, n = release exponent.

Table 8: Actual quantities for the optimization of the liquisolid tablets

Run (batch)	Independent Factors		Dependent factors	
	Concentration of non-volatile solvent	Carrier: coat ratio (R)	Drug release (%)	Drug content (%)
1	100	5	84.70 ± 0.00	97.1 ± 1.59
2*	100	5	86.60 ± 1.20	97.4 ± 0.07
3	100	5	82.25 ± 1.44	96.9 ± 0.38
4	200	5	81.55 ± 0.95	97.0 ± 0.15
5	200	5	83.35 ± 0.17	96.7 ± 0.42
6	200	5	83.90 ± 0.56	95.9 ± 0.65
7	300	5	81.65 ± 1.02	96.3 ± 0.31
8	300	5	83.30 ± 0.42	95.4 ± 0.65
9	300	5	85.35 ± 0.74	96.9 ± 0.58
10	400	5	82.25 ± 0.31	95.9 ± 0.40
11	400	5	83.70 ± 0.42	96.1 ± 0.90
12	400	5	84.40 ± 0.91	95.7 ± 0.74

*The batch that was selected for optimization

Table 9: Formulation design of celecoxib liquisolid tablets

Formulation code	Non-volatile liquid vehicle (mg)	R	Drug: liquid vehicle ratio	Active ingredients (mg)	Liquid vehicle (mg)	Lf	Carrier (mg)	Coating material (mg)	Starch (5%)	Mag. Stearate (1% total weight, mg)	Total weight (mg)
F-2	PEG-400	5		100		0.46	434.8	87.5	33.77	6.754	675.4
CT	----	----	----	100	----	----	425.7	85.1	30.54	6.108	610.8

R: Carrier and coating material ratio, Lf: Liquid load factor, Q; W/Lf (Q = carrier material and W: Total weight of drug and liquid vehicle), q = Q/R (q = coating material), CT: Conventional tablet without the non-volatile vehicle.
Carrier material: F-2, CT: lactose, Coating material: F-2, CT: Silicon dioxide (SiO_2)
Disintegrant: F-2, CT: Maize starch

Formular Development for Optimized Liquisolid Tablet

The optimized formulation was selected based on the results obtained for dependent variables *(in vitro* drug release and drug content). From the results obtained, batch F-2 had the highest drug content of 97.4 ± 0.07 with percentage drug release of 86.60 ± 1.20.

Pre-Compression Studies of the Optimized Formulation

The angle of repose is a characteristic of the internal cohesion of the particles. If a powder is non-cohesive, the angle of repose will be high, but if a powder is cohesive, the angle of repose will be low (ASTM International, 2014). The angle of repose of the optimized formulation was 22.10 ± 1.21, while that of the conventional tablet was 23.32 ± 0.35 without a significant difference ($p < 0.05$).

The bulk density of the optimized formulation was 0.21 ± 0.02, while that of the conventional tablet was 0.22 ± 0.01. The tapped density of the optimized formulation was 0.25 ± 0.01, while that of the conventional tablet was 0.34 ± 0.01. The Hausner ratio of the optimized formulation was 1.24 ± 0.03, while that of the conventional tablet was 1.14 ± 0.02. The Carrs index of the optimized formulation was 20.17 ± 1.40, while that of the conventional tablet was 18.00 ± 0.36. The drug content of the optimized formulation was 97.4 ± 0.07, while that of the conventional tablet was 95.7 ± 0.98, without a significant difference ($p < 0.05$).

Table 10: pre-compression parameters of optimized liquisolid granules of Celecoxib (n =3, all values are written as Mean ± SD)

Pure drug/codes	Angle of repose (^{o})	Bulk density (g/ml)	Tapped density (g/ml)	Hausners Ratio	Compressibility index (%)
F-2	22.10 ± 1.21	0.25 ± 0.01	0.25 ± 0.01	1.14 ± 0.02	20.17± 1.40
CT	23.32 ± 0.35	0.22 ± 0.01	0.34 ± 0.01	1.27 ± 0.04	18.00 ± 0.36

Post Compression Evaluation of the Optimized Formulation

The general appearance of the tablets were white. The hardness of the optimized formulation was 4.90 ± 0.56, while that of the conventional tablet and the reference commercial tablet were 4.50 ± 0.21 and 4.85 ± 0.60 respectively. The thickness of the optimized formulation was 4.60 ± 0.21, while that of CT and RCT were 4.45 ± 0.21 and 3.80 ± 0.61 respectively. The diameter of the optimized formulation was 5.14 ± 0.28, while that of the CT and RCT were 4.45 ± 0.30 and 4.56 ± 0.31 respectively. The friability of the optimized formulation was 0.59 ± 0.08, while that of the CT and RCT were 0.45 ± 0.01 and 0.41 ± 0.01 respectively. The disintegration time of the optimized formulation was 5.02 ± 0.17, while that of the CT and RCT were 12.30 ± 0.14 and 12.38 ± 0.21 respectively.

Table 11: Post compression evaluation of the optimized formulation, conventional tablet and reference commercial tablet of Celecoxib (mean ± SD)

Formulation code	General appearance	Hardness (kg/cm^2)	Thickness (mm)	Diameter (mm)	Weight variation (mg)	Friability (%)	Disintegration time (sec)
F-2	White	4.90 ± 0.56	4.60 ± 0.21	5.15 ± 0.29	677.40± 1.62	0.59 ± 0.08	5.45 ± 0.17
CT	White	4.50 ± 0.21	4.50 ± 0.21	4.45 ± 0.17	606.90 ± 2.75	0.50 ± 0.00	13.30 ± 0.14
RCT	White	3.85 ± 0.60	3.85 ± 0.60	4.56 ± 0.32	600.70 ± 2.80	0.40 ± 0.00	12.40 ± 0.21

Carrier material: Lactose, Coating material: silicon dioxide, Disintegrant: maize starch

In vitro release studies of the optimized formulation, conventional tablet and reference commercial tablet.

In vitro dissolution studies were carried out by USP type II method by using 0.1 N HCl as the dissolution medium. The studies were performed in all the formulations for 1 hour. The samples were taken at 5 minutes interval for first 30 minutes and 15 minutes interval for next 30 minutes and absorbance was measured in UV spectrophotometer at 354 nm. Two formulation parameters that normally affect the drug dissolution rate in immediate release liquisolid tablets were investigated. They include the effect of drug concentration in the liquid medication (ratio of drug and liquid vehicle) and effect of carrier/coating ratio (R-value). The results of the *in vitro* release studies of optimized formulation, conventional tablet and reference commercial tablet are shown in Table 12. At 1 hour 88.4 ± 1.20, 76.40 ±0.74, 65.60 ± 0.28 were released by the optimized formulation, conventional tablet and reference commercial tablet respectively.

Table 12: In-vitro release profile of the optimized formulation, conventional tablet and reference commercial tablet (mean ± SD)

Time (min)	Dissolution medium	F-3	F-CT	RCT
0	0.1 N HCl	0	0	0
5		34.2 ± 0.56	36.10 ± 0.42	24.90 ± 0.21
10		44.0 ± 1.69	46.85 ± 0.24	36.30 ± 0.28
15		56.0 ± 0.07	50.00 ± 0.01	45.05 ± 0.24
20		63.0 ± 0.63	56.95 ± 0.88	48.85 ± 0.03
25		69.0 ± 0.28	65.30 ± 0.14	54.80 ± 0.21
30		74.0 ± 0.21	68.50 ± 0.14	58.85 ± 0.74
45		83.0 ± 0.14	70.30 ± 0.41	62.90 ± 0.21
60		88.4 ± 1.20	76.40 ±0.74	65.60 ± 0.28

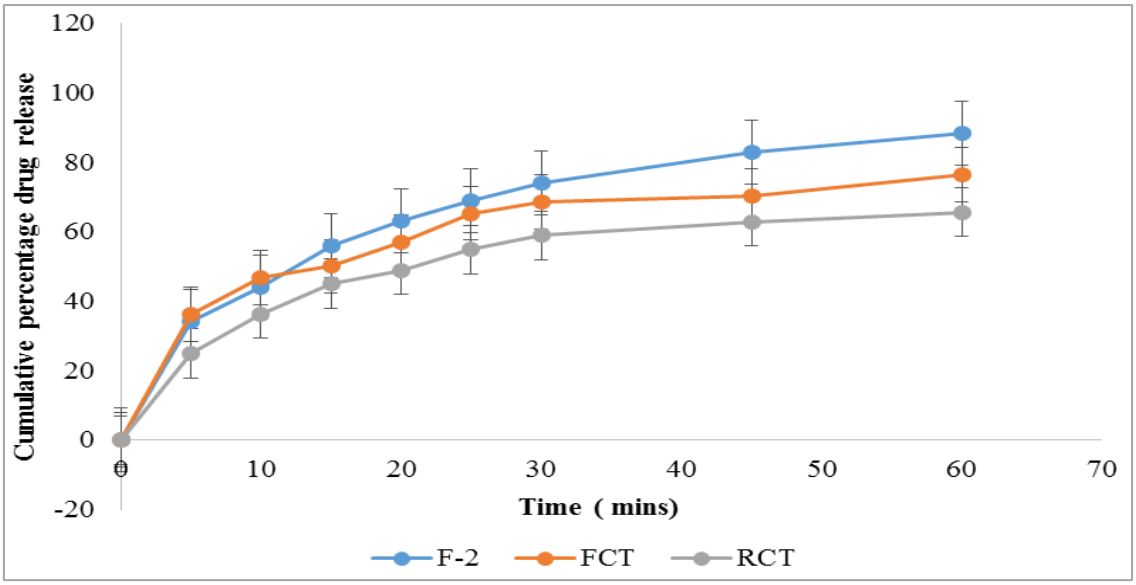

Figure 13: Cumulative percentage drug release of optimized batch (F-3), conventional tablet and reference commercial

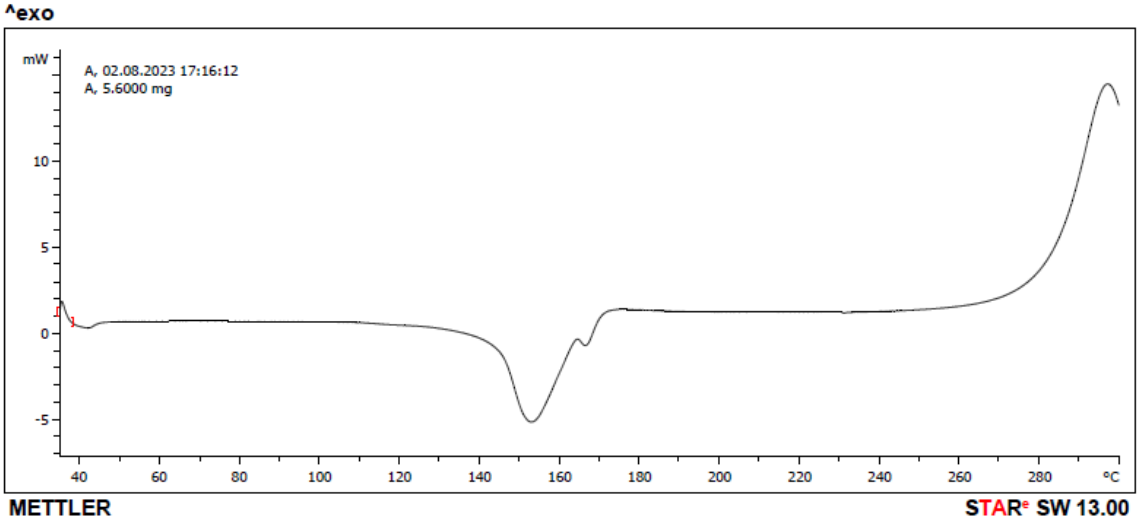

Figure 14: DSC thermogram of Celecoxib

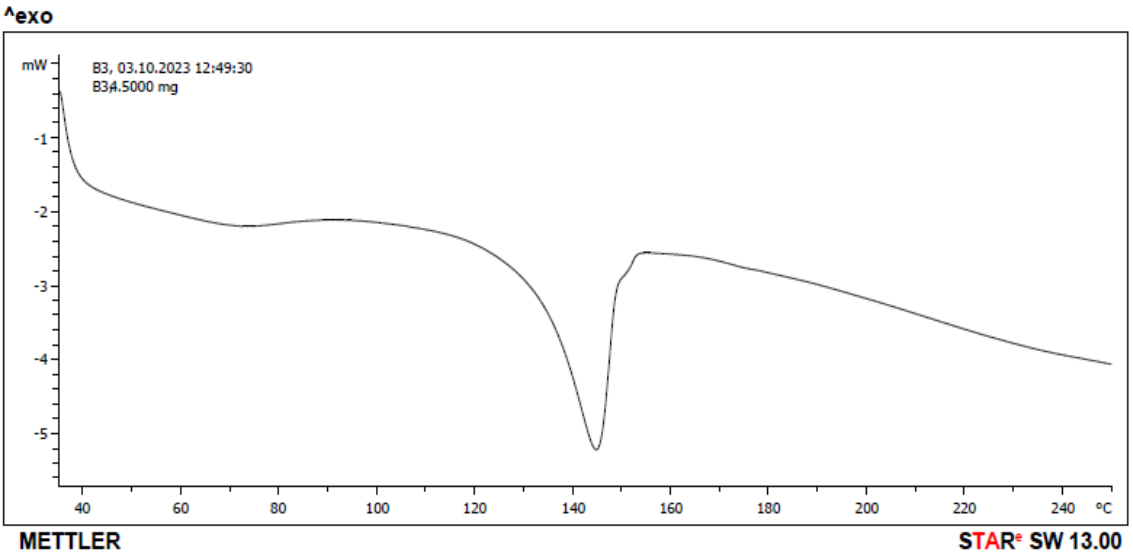

Figure 15: DSC thermogram of Celecoxib and lactose

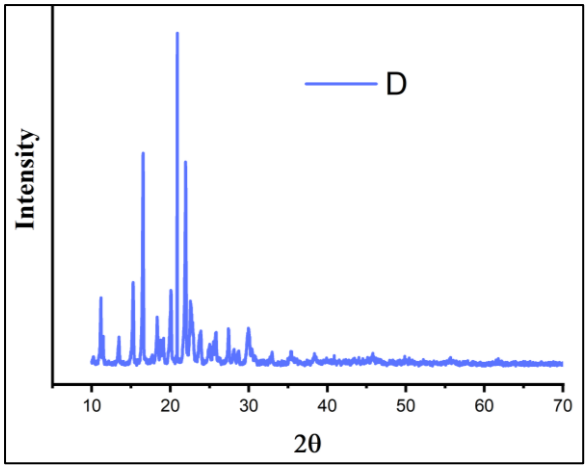

Figure 16: XRD of celecoxib

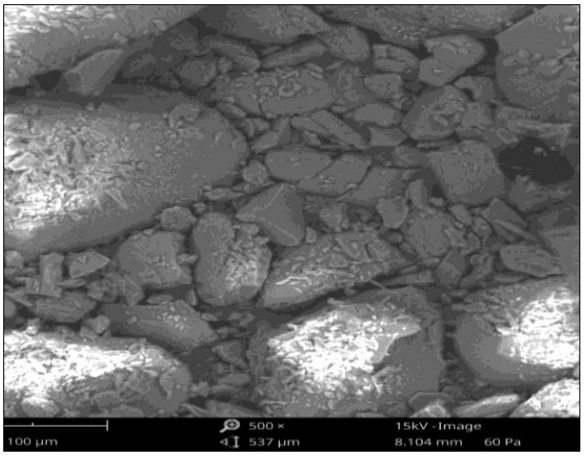

Figure 17: SEM photograph of optimized formulation of celecoxib

CONCLUSION

The results demonstrated significant improvements in the solubility, dissolution rate and bioavailability of celecoxib liquisolid compacts. These findings suggested that the liquisolid technique is a promising approach for improving the bioavailability of poorly water-soluble drugs like celecoxib. The developed liquisolid compacts have the potential to enhance the therapeutic efficacy of celecoxib, and further i*n vivo* studies are warranted to confirm these findings.

Abbreviations

FTIR: Fourier transform infra-red

SEM: Scanning electron microscopy

PEG: Polyethylene glycol

KBR: Potassium bromide

REFERENCES

Abdullah A., Chalimah S., Primadone I. and Hanantyo M., 2018. Physical and chemical properties of corn, cassava and potato starches. Earth and Environmental Science, **160**: 12-30.

Allen T.M. and Cullis P.R., 2004. Drug delivery systems: entering the mainstream. Science, **303**(5665): 1818-1822.

Amidon G.L., Lennernäs H., Shah V. P. and Crison J.R., 1995. A theoretical basis for a biopharmaceutic drug classification: the correlation of in vitro drug product dissolution and in vivo bioavailability. Pharmaceutical Research, **12**(3): 413-420.

ASTM International, 2013. ASTM B213-13: standard test methods for flow rate of metal powders using the hall flow meter funnel. ASTM_International, West Conshohocken, PA.

ASTM International, 2014. ASTM F3049-14: Standard guide for characterizing properties of metal powders used for additive manufacturing processes. ASTM_International, West Conshohocken, PA.

Ankit B., Rathore R.P.S., Tanwar Y.S., Gupta S. and Bhaduka G., 2013. Oral sustained release dosage form: an opportunity to prolong the release of drug. I.J.A.R.P.B., **3**(1): 7-14.

Akinlade B., Elkordy A.A., Essa E.A. and Elhagar S., 2010. Liquisolid systems to improve the dissolution of furosemide. Scientia pharmaceutica, **78**(2): 325.

Asare-Addo K., Conway B.R., Hajamohaideen M.J., Kaialy W., Nokhodchi A. and Larhrib H., 2013. Aqueous and hydro-alcoholic media effects on polyols. Colloids Surfaces B Biointerfaces, **11**(1): 9–24.

Alireza H., Fatemeh S., Ali N., Jaleh V. and Hadi A., 2015. Preparation and characterization of celecoxib dispersions in Soluplus: comparison of spray drying and conventional methods. Iranian Journal of Pharmaceutical Research, **14**(1): 33-50.

Armstrong N.A., 2006. Tablet manufacture. In: Swarbrick J, Boylan JC, editors. Encyclopedia of pharmaceutical technology. 3rd Edition. New York: Marcel Dekker.

Badawy M.A., Kamel A.O. and Sammour O.A., 2016. Use of biorelevant media for assessment of a poorly soluble weakly basic drug in the form of liquisolid compacts: in vitro and in vivo study. Drug Delivery, **23**(3): 808-817.

Baveja S.K., Ranga Rao K.V. and Padmalatha Devi K.,

1987. Zero-order release hydrophilic matrix tablets of adrenergic blockers. Int. J. Pharm., **39**(1–2): 39–45.

Bettini R., Catellani P.L., Santi P., Massimo G., Peppas N.A. and Colombo P., 2001. Translocation of drug particles in HPMC matrix gel layer: effect of drug solubility and influence on release rate. Journal of Controlled Release, **70**(3): 383-391.

Beignon M., Bohic S., Le Guennec M., Le Goff D., Roger P. and Proutire A., 1998. Molecular weight determination of macromolecules with a new simplified and coherent light scattering method. J. Mol. Struct., **443**(1–3): 233–53.

Blagden N., de Matas M., Gavan P.T. and York P., 2007. Crystal engineering of active pharmaceutical ingredients to improve solubility and dissolution rates. Adv. Drug Deliv. Rev., **59**(7): 617–30.

Chuahan P.V., Patel H.K., Patel B.A., Patel K.N. and Patel P.A., 2012. Liquisolid technique for enhancement of dissolution rate of ibuprofen. International Journal for Pharmaceutical Research Scholars, **1**(1): 268-280.

Dorozynski R., Jachowicz P., Kulinowaski S., Kwiecinski, Szybinski K. and Skora T., 2004. The macromolecular polymers for the preparation of hydrodynamic ally balanced system-methods of evaluation. Drug Dev. Int. Pharm., **30**(9): 947-957.

Farheen F., Sharma G., Rathore A. and Sharma N., 2015. Liquisolid technology: A review. World Journal of Pharmacy and Pharmaceutical Sciences, **2**(3): 947-958.

Gulshan M., Lakshmi Swapna Sai M., Rajesh J. and Rama Rao N., 2016. A novel formulation of celecoxib in the treatment of familial adenomatous polyposis. J. Global Trends Pharm. Sci., **7**: 3004-8.

Hoffman A., David S., Eran L., Sara R., Eytan K. and Ichael F., 2004. Pharmacokinetic and pharmacodynamic aspects of gastro retentive dosage forms. Int. J. Pharm., **277**: 141-153.

Kaur M., Bala R. and Arora S., 2013. Liquisolid technology: A review. An International Journal of Advances in Pharmaceutical Sciences, **4**(1):1-15.

McCormack P.L., 2011. "Celecoxib: a review of its use for symptomatic relief in the treatment of osteoarthritis, rheumatoid arthritis and ankylosing spondylitis". Drugs, **71**(18): 2457-89.

Modi A. and Tayade P., 2006. Enhancement of Dissolution Profile by Solid Dispersion (Kneading) Technique. AAPS Pharm Sci. Tech., **7**(3): Article. DOI: 10.1208/pt070368.

National Institute for Health and Care Excellence (NICE). Non-steroidal anti-inflammatory drugs. Manchester: NICE; 2013. Available from: www.nice.org.uk (Accessed Sep, 2013).

Nafiseh M.N., Javad S., Nasimi N., Ali R.Z., Matthew L. and Yousef J., 2022. Combining liquisolid and co-grinding techniques to enhance the dissolution rate of celecoxib. Journal of Pharmaceutical Innovation, **18**: 300-309.

Ning J., Shu M., Ming G., Jie F. and Run C., 2011. Synthesis and characterization of cellulose-silica composite fiber in ethanol/water mixed solvents. Bioresources, pp.1186-1195.

Sahil M.G., Sharad S.P., Shirish V.S., Kisan R.J. and Vilasrao J.K., 2018. Liquisolid Compact: A New Technique for Enhancement of Drug Dissolution. International Journal of Research in Pharmacy and Chemistry, **3**(1):705-715.

Saravanan S. and Dubey R., 2020. Synthesis of SiO_2 nanoparticles by Sol-Gel method and their optical and structural properties. Romanian Journal of Information Science and Technology, **23**(1): 105-112.

Sue H., Tamar Z., Irith G., Jackie K. and Abraham R., 2006. Luminal delivery and dosing considerations of local celecoxib administration to colorectal cancer. Eur. J. Pharm Sci., **28**: 204-11.

Syed I. and Pavani E., 2012. A Review on The Liquisolid Technique Based Drug Delivery System. International Journal of Pharmaceutical Sciences and Drug Research, **4**(2): 88-96.

Utsav S.P. and Khushbu C.P., 2018. Liquisolid Technique for Poorly Soluble Drugs. Journal of Science and Innovative Research, **2**(1): 145-159.